Measurement of Displacement Around Holes in Composite Plates Subjected to Quasi-Static Compression

John C. Duke, Jr., Daniel Post,
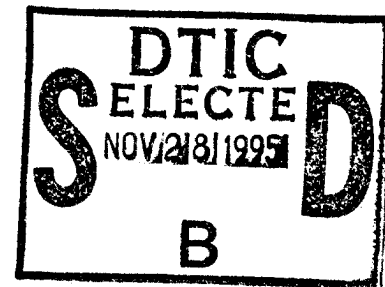Robert Czarnek, and Anand Asundi

NASA

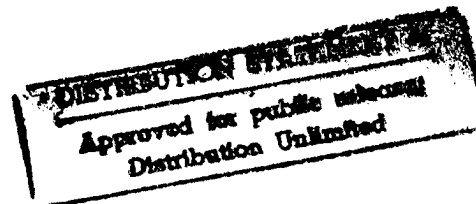NASA Contractor Report 3989

Measurement of Displacement Around Holes in Composite Plates Subjected to Quasi-Static Compression

John C. Duke, Jr., Daniel Post,
Robert Czarnek, and Anand Asundi

Virginia Polytechnic Institute and State University
Blacksburg, Virginia

NASA

National Aeronautics
and Space Administration

**Scientific and Technical
Information Branch**

1986

Table of Contents

MEASUREMENT OF DISPLACEMENT AROUND HOLES
IN COMPOSITE PLATES SUBJECTED TO QUASI-STATIC COMPRESSION

BY

John C. Duke, Jr., Daniel Post,
Robert Czarnek, and Anand Asundi

Virginia Polytechnic Institute and State University
Blacksburg, Virginia

ABSTRACT

Contour maps of thickness changes were obtained for three quasi-isotropic graphite-epoxy plates with central holes, loaded in compression. Thickness changes were determined for six load increments from nearly zero to within a few percent of the failure load. The largest change of thickness occurred near the hole but not at the boundary of the hole. Below 90% of the failure load, the thickness changes were nearly proportional to load. Irregularities of thickness changes occurred in zones of compressive stresses and they were attributed to localized fiber buckling.

A new optical technique was developed to measure thickness changes with high sensitivity. It utilizes a comparatively simple means of holographic interferometry on both sides of the specimen, followed by additive moire to obtain thickness changes as the sum of the out-of-plane displacements. Sensitivity was 12.5×10^{-6} in. per fringe order. The fringe patterns represent thickness changes uniquely, even when specimen warpage and consequent out-of-plane displacements are very large.

INTRODUCTION

This study is part of a continuing exploration of the structural behavior of fiber-reinforced composite materials by NASA (Langley). The dual purposes of the present research are to

(1) develop a whole-field, high-sensitivity optical technique to measure load-induced changes of thickness of composite plates, and

(2) measure changes of thickness of three composite plates, each with a central hole of different prescribed size, as a function of applied compressive loads.

The specimens were graphite-epoxy plates of quasi-isotropic layup, having dimensions shown in Fig. 1. They were supplied by NASA.

OPTICAL METHOD

Basic Approach

When external loads are applied to a plate, its thickness changes and its surfaces experience out-of-plane displacements W_I and W_{II}, as illustrated in Fig. 2. In general these changes vary across the plate as a function of x and y.

In the scheme developed here for thickness change measurements, a variation of holographic interferometry is used first to produce whole-field contour maps of W_I and W_{II}. Its sensitivity is $\lambda/2$ displacement per fringe order (or contour level) of the contour map. At any point x,y in the specimen,

$$W_I = \frac{\lambda}{2} N_I \; ; \; W_{II} = \frac{\lambda}{2} N_{II} \tag{1}$$

where λ is the wavelength used to construct the hologram and

N_I, N_{II} are fringe orders at that point in the reconstructed

holographic interferometry patterns from faces I and II,

respectively.

Of course, the total thickness change, ΔT, at any point x,y is

$$\Delta T = W_I + W_{II} = \frac{\lambda}{2} (N_I + N_{II}) \tag{2}$$

The method would be most effective if the patterns from the two faces are combined into a single contour map of ΔT. While it is better known that contour maps can be subtracted by moire methods, moire can be used to add contour maps, too.

In the present method, carrier patterns of equal frequencies and opposite signs are added to the fringe patterns. Fringe orders at any point x,y are thereby changed to $N_I + N_C$ and $N_{II} - N_C$, where N_C represents the fringe order attributable to the carrier pattern. When these two contour maps are superimposed, they interweave to form a moire pattern of the additive parameter, N, where

$$N = (N_I + N_C) + (N_{II} - N_C) = N_I + N_{II} \tag{3}$$

Equations (2) and (3) combine to show that the moire fringe order at each point x,y is proportional to the thickness change at that point by

$$\Delta T = \frac{\lambda}{2} N \qquad\qquad (4)$$

Optical filtering is used to enhance contrast of the moire pattern, thus producing a clear contour map of thickness changes throughout the field of view.

The final contour map gives relative values of ΔT, however, and it is necessary to know the absolute value of ΔT at some point in the field of view to assign absolute values throughout the field. This is accomplished by a rather simple optical clip gage attached to the specimen.

Whereas holographic interferometry is usually conducted with specimens that produce matte (or diffuse) reflection of light, [1,2] the specimens used in this study were prepared with smooth, specularly reflecting faces. Accordingly, the problems associated with speckles, including speckle correlation and loss of fringe contrast, encountered with matte surfaces in holographic interferometry were circumvented.

The optical method is described in greater detail in the following sections.

EXPERIMENTAL PROCEDURE

Nondestructive Examination

Upon receipt of the specimens each was examined nondestructively by pulse echo ultrasonic C-scanning. The quality of the three specimens used for the change of thickness measurements appears to be typical of structurally sound panels.

Specimen Preparation

The specimens were prepared with smooth mirrorized coatings. First, a thin layer of room-temperature curing epoxy was cast on each face, using the smooth surface of a thin Plexiglass plate as an external mold. Ultra-thin aluminum was coated on the smooth epoxy by vacuum deposition.

Loading

Each specimen was loaded in compression, using a NASA fixture to engage its perimeter and prevent buckling. A Tinius Olsen testing machine of 120,000 pounds capacity was used. A spherical seat on the upper loading anvil was adjusted to produce nearly uniform loading across the width and thickness of the specimen, as indicated by four electric strain gages on the specimen (Fig. 1). The adjustment was made at approximately 15,000 pounds compressive load and it was maintained by friction in the spherical seat for the remainder of the test. The load was reduced to about 1000 pounds to begin the test sequence.

Holograms were made for load increments of approximately 15,000 pounds up to about 70% of maximum load. Then, increments were reduced gradually to 3000 pounds near anticipated failure of the specimen. Strain gage data was taken for each load increment to assess load uniformity.

Hologram Exposures

The basic experimental data was obtained by reflection-type holographic interferometry. For this, the fixture shown in Fig. 3 was used to hold a high resolution photographic plate adjacent to each mirrorized surface of the specimen. The specimen and photographic plates were illuminated from each side by the dual optical system illustrated in Fig. 4a. Light from the

expanded and collimated laser beam passed through the photographic emulsion (Fig. 4b), reflected back from the specimen surface, and penetrated the emulsion again. Thus, the emulsion was exposed simultaneously to two coherent beams with wavefronts WF_1 and WF_2, which interacted to produce a stationary pattern of interference fringes. The beam with WF_1 is the reference beam while that with WF_2 is the information beam.

The fringes lie along the bisector of the wavefronts, forming adjacent planes or walls of constructive and destructive interference nearly parallel to the specimen surface. About 60 such walls are produced within the small thickness (approximately 13 microns) of the emulsion.

A double exposure is made for each load increment. After the first exposure,

(1) The photographic plates are inclined through an identical small angle to create the carrier pattern. This is done by advancing the micrometer screw on the holographic plate fixture (Fig. 3). Then

(2) the specimen is loaded in compression to a predetermined load, and

(3) the second holographic exposures are made on the same photographic plates.

These exposures are made in a dark enclosure -- a light-tight polyethelene enclosure built around the testing machine. After each load increment, the photographic plates are removed, fresh plates are installed and the steps are repeated for another increment of compressive load, with the sequence continuing until the breaking load is reached.

Reconstruction

Each photographic plate contains two interweaving systems of interference, as illustrated with exaggerated angles in Fig. 5. The light

reflecting back from the surface of the specimen does not have a plane wavefront, but instead it has a warped wavefront with warpage twice that of the mirrorized specimen surface. Consequently, the walls of constructive interference are warped in harmony with the specimen warpage. The photographic plate -- now called a hologram -- contains complete information on the out-of-plane warpage of the specimen before and after the load increment. In addition, this information is separated by the small ($\approx 1/3°$) constant angle introduced between exposures.

After development, the photographic emulsion is comprised of partially transparent walls of silver in the zones of constructive interference, separated by clear walls of gelatin lying in the zones of destructive interference. These silver walls act as partial mirrors -- internal mirrors in the volume of the emulsion. Upon reconstruction, light is reflected at the successive mirrors as shown for only one system at the top of Fig. 6. The optical path length between these adjacent mirror walls is half a wavelength, so each emergent contribution is one wavelength out-of-phase with its neighbors. The result is constructive interference between all these contributions, producing a reasonably strong reflection.

Three beams emerge from the hologram: a beam from the glass/emulsion interface (and glass/air interface), which is wasted; and two beams from the internal mirrors which carry the desired information and are collected by the observer.

The optical system for reconstruction is illustrated in Fig. 7. A convergent beam of laser light illuminates the hologram through action of a beam-splitter. The two information beams converge to small zones in the plane of the camera aperture and they are admitted into the camera. The third beam from the hologram surface emerges in a different direction and it is stopped

by the aperture; note that this is the reason for the inclination of the photographic plate shown in Figs. 4-6. The two information beams that reflect from the internal mirrors of the hologram have warped wavefronts and the camera photographs the interference pattern generated by interaction of these two coherent beams.

The interference pattern is a contour map of the separation or gap, s, between the wavefronts (in the object plane or specimen plane of the hologram). This is illustrated schematically and greatly exaggerated in Fig. 8a, where the two wavefronts have different shapes since they represent different states of specimen deformation. Furthermore, the two wavefronts exhibit a general inclination with respect to each other (shown by dashed lines), corresponding to the change in inclination of the holographic plate introduced between the exposures.

If the two wavefronts had identical warpage, the contour map of s would be parallel equally spaced fringes induced by the inclination alone. This uniform fringe gradient is called a carrier pattern. In the actual event, information depicting the difference of warpage on the two wavefronts is introduced as variations in the otherwise regular carrier pattern, as sketched in Fig. 8b.

Accordingly, at any specimen point x,y, the fringe order M in Fig. 8b is the sum of the fringe orders attributable to the wavefront warpage and the carrier pattern. For Face I this is

$$M_I = N_I + N_{cI} \tag{5}$$

and for Face II

$$M_{II} = N_{II} + N_{cII} \tag{6}$$

Alternative Explanation

In the argument presented here, the wavefronts of light emerging from the hologram in the reconstruction step are identical to those striking the photographic plate in the hologram construction step. However, this does not account for the fact that the emulsion of the photographic plate shrinks in thickness as a result of processing. After processing, the distance between internal mirrors (Fig. 6) is less than the distance between walls of constructive interference of the exposure (Fig. 4). Thus, constructive interference of contributions from each partial mirror occurs for a shorter wavelength. At the same time, warpage of the internal mirrors is diminished uniformly across the hologram by the same proportion. As a result, the wavefront warpage will produce exactly the same interference pattern with the shorter wavelength as an unshrunken hologram would produce with the original wavelength.

This suggests that precisely the right shorter wavelength must be used to obtain a correct pattern of W displacements. In practice, however, the contour map produced by reconstruction is unique, while its intensity is influenced by the wavelength of reconstruction. The following alternative explanation of reconstruction supports this.

Consider the zone near AA in Fig. 5. Walls of constructive interference from exposures 1 and 2 are superimposed; after development, successive partial mirrors of silver reflect light in the reconstruction process. Along BB, however, the walls of constructive interference of exposure 2 fall exactly between those of exposure 1. Since the intensities of the individual interference patterns are harmonic, the two intensities with a half-cycle shift sum to a constant value across BB. Near BB there are no partial mirror surfaces and no directed light reflects from the interior of the emulsion.

8

The positions of these zones of reflectivity (AA) and non-reflectivity (BB) correspond to the positions of constructive and destructive interference viewed in the camera. Since emulsion shrinkage does not alter the positions of zones AA and BB, the resultant pattern is independent of shrinkage.

In this work, red light of helium-neon lasers (λ = 24.9 μin or 633 nm) was used to produce the holograms. After processing, reflection of green light was strongest and green light of an argon laser (λ = 20.2 μin or 514 nm) was used for reconstruction.

Summation by Moire and Optical Filtering

Two films with patterns corresponding to Fig. 8b are produced by reconstruction, one from each side of the specimen. Their superposition produces a moire pattern and, in order to support Eqs. (3) and (4), it remains to show that this is a pattern of $N_I + N_{II}$.

Let the y-axis correspond to the axis of rotation of the fixture carrying the two holographic plates (Fig. 2). With this linkage, the change of gap between specimen and hologram, caused by rotation of the fixture, is exactly equal and opposite for every corresponding point x,y on Faces I and II. Therefore, fringe orders attributable to the carrier pattern are exactly opposite and Eqs. (5) and (6) may be written

$$M_I = N_I + N_c \; ; \; M_{II} = N_{II} - N_c \tag{7}$$

It is well established [3] that superposition of two contour maps with contours of M_I and M_{II} produces a moire pattern in which the subtractive parameter $M_{II} - M_I$ and the additive parameter $M_{II} + M_I$ are both present. Only one of the two parameters emerges with good visibility.

9

In the present case, superposition of the two reconstructed holograms, namely, superposition of contours M_I and M_{II}, produces the subtractive moire

$$M_{II} - M_I = N_{II} - N_I - 2N_c \tag{8}$$

and the additive moire

$$M_{II} + M_I = N_{II} + N_I \tag{9}$$

Since the carrier pattern is adjusted to dominate, N_c is large compared to $N_{II} - N_I$; the subtractive moire has very closely spaced fringes, with the general appearance of Fig. 8b. The additive moire has relatively few fringes across the field of view, and these moire fringes appear with good visibility on a background of the subtractive moire field. In this case, because carrier patterns of opposite signs were used, superposition yields the additive moire of Eq. (9).

When the films from hologram reconstructions of Faces I and II are superimposed, the moire fringes have the general appearance shown in Fig. 9a. Broad zones of continuous black areas are formed where dark and light bands interweave. Elsewhere, striped zones remain.

Figure 9b illustrates a simple means of further enhancing contrast of the additive moire pattern by optical filtering. When the superimposed films are inserted into this arrangement, the striped zones diffract light into many diffraction orders. The camera aperture is adjusted to accept light from the first diffraction order only, thus projecting uniform bright bands of light into the image plane from the striped zones on the object.

Sensitivity

By Eq. 4, the sensitivity is $\lambda/2$ change of thickness per fringe order, in the final moire pattern, where λ is the wavelength used to produce the hologram. Here, λ is 24.9 μin. (633 nm) and the sensitivity is 12.5 μin. (317

10

nm) per fringe order. The load-induced change of specimen thickness is constant along a continuous fringe, and its magnitude changes by 12.5 μin. in the zone between neighboring fringes.

Absolute Thickness Change

While the pattern of N is a contour map of thickness change, it does not necessarily reveal the absolute value of N at any point. For complete information, the absolute value of N at some point must be known from subsidiary information. In many cases it is known from the geometry of the specimen; an example is the case of a specimen with an unloaded external corner, where the stresses are all zero and $\Delta T = N = 0$. In the present case, however, it was necessary to measure the absolute value of ΔT at one point in the field to establish the absolute value of N throughout the field. An optical clip gage was used for the purpose.

Optical Clip Gage

The optical clip gage is illustrated in Fig. 10. It consists of two plates held by friction against the specimen by the force of spring wires. Plate I engages the specimen at three points; Plate II engages it at two points along the bottom while the top engages an adjustable leg extending from Plate I. Thin glass mirrors are attached to the surface of each plate. In operation, the separation between the mirror surfaces remained fixed at the top opposite the upper contact point. At each leg along the bottom, the mirror separation changed by an amount equal to the change of thickness of the underlying specimen.

The fringe pattern seen on the clip gage represents contours of its change of separation. The change is zero opposite the top leg and the

absolute fringe order there is zero. The fringe orders change monotonically and their values can be counted and determined at the locations of each leg at the bottom. Of course, the fringes at corresponding points on the specimen must have the same absolute fringe order.

CAUTION: TEMPERATURE EFFECTS

Development of this method was frustrated by extraneous fringes in the change of thickness patterns. Concentric circular fringes were found even when no load was applied to the specimen. Their presence was traced to temperature effects in the holographic plates.

When a 4 x 5 x 0.040 inch photographic plate was removed from its box, it was carried with its emulsion side close to the palm of the hand and the hand warmed that side. While it was being installed in the fixture shown in Fig. 3, the close proximity of the hands continued to warm the same side. The resultant temperature gradient through the plate thickness causes a spherical curvature of the plate, which relaxed with time as the temperature gradient diminished.

The extraneous fringes were caused by the change of spherical shape that occurred in the time interval between the first and second holographic exposures. Holography measures the change of gap (or optical path length) between the specimen and the plate and responds equally to changes in either one. Calculations showed that a change in temperature gradient of only a fraction of one degree is sufficient to introduce several fringes in the thin plate.

The temperature gradients were also responsible for another defect in earlier tests--the absence of fringes and low contrast of fringes in portions of some patterns. If the path length between the specimen and the

12

photographic plate changes by 1/4 of a wavelength, or 6μin., during the exposure time (about 10 seconds), constructive interference in the hologram changes to destructive interference and destroys the fringes of the hologram. Such motions must have occurred in earlier tests; the absence of fringes is attributed to heat dissipation from the warmed surface of the plate and corresponding relaxation of stresses during the holographic exposure time.

Several steps were taken to solve the problem. The photographic plates were cemented to 1/4 inch thick glass plates with a transparent epoxy adhesive. Besides having a higher thermal capacity, the strain per unit temperature gradient is much less for thicker plates. Thick photographic plates are commercially available, but the lamination was a satisfactory and economical substitute. In addition, the plates were handled with gloves to minimize heat transfer; they were handled with the fingertips and not placed in close proximity to the palm of the hand; and several minutes were allowed to elapse between installing the plates in the fixture and taking the first exposure.

This temperature effect was unexpected and surprising. It brings to mind the question of whether numerous other experiments and measurements in the literature of holographic interferometry may have experienced similar extraneous effects.

EXPERIMENTAL RESULTS

The results of the three tests performed in this study are presented in the figures and tables. For each pair of holograms, the load levels and associated strain gage readings are presented in tabular form in Tables 1-3. Fringe patterns, or contour maps of thickness changes, are shown for each load increment to near failure. Figures 11, 12, and 13 display patterns for the

3/4, 1/2 and 1/4 inch hole specimens, respectively. The figure captions indicate the nominal load magnitudes, which are within a fraction of a percent of the measured values given in Tables 1-3. Selected patterns are labeled with fringe order numbers. Individual and accumulated thickness changes that occurred at the horizontal midplane are presented in Figs. 14, 15 and 16; thickness changes along the perimeter of the 3/4 inch hole are shown in Fig. 14c. Where graphs show only fringe orders N, thickness changes may be calculated as $\Delta T = (12.5 \times 10^{-6} \text{ in.})(N)$.

The maximum value of thickness changes in the vicinity of the hole is plotted as a function of load in Figs. 17 a, b and c. These graphs offer an indication of very modest non-linear behavior up to very high load levels, and increased non-linearity near failure. For most data points on these graphs, the peak fringe orders on the left and right sides of the hole were virtually equal and the two plotted points appear as one. For others, both data points are shown and the graph is drawn midway through them.

Calculation of Change in Thickness at a Point

The following procedure was followed to calculate the absolute change in thickness at any point in the field of view. For each pattern, the fringe order in the clip gage at its specimen contact points was counted, assuming zero order at the center of the rigid spacer. The contour line of specimen thickness that passed through the contact point was assigned the same fringe order. Then, the surrounding fringes were enumerated by the rules of topography and casual knowledge of the nature of deformation for such a specimen.

At any point, the total change of thickness after the ith load increment is given by

$$\Delta T_i = \left(N_1 + N_2 + \text{---} + N_i \right) \frac{\lambda}{2} \qquad (10)$$

where N_1, N_2, ---, represent fringe orders at the given point for each step of the loading sequence. The accumulated thickness changes shown in Figs. 14-16 were determined by this procedure.

DISCUSSION OF RESULTS

The three specimens all failed at loads close to those predicted by NASA. Very large out-of-plane distortions were noticed for the specimen with a 1/4 inch hole, while the distortions observed at high load levels were much less for the other two specimens.

Fringes in the region of dominant tension above and below the holes are relatively smooth, while fringes in all other regions indicate irregular small variations of thickness from point-to-point along the specimen. It is speculated that local material instabilities, or localized fiber buckling, causes these irregularities in the compression zones.

The general character of the thickness change patterns is similar to those for isotropic materials, but with one distinct difference. With isotropic materials, the thickness change along the horizontal centerline increases monotonically to a peak at the hole boundary. In contrast, these quasi-isotropic composite specimens reveal a plateau in the thickness change near the hole boundary, and in most cases they reveal a dropoff immediately adjacent to the boundary.

Additional details of each test are discussed below.

3/4 Inch Hole

Curiously, the specimen exhibited severe in-plane bending during load increment no. II, and bending of opposite sign for increment no. III. One may note that the strain gage readings do not reveal the large magnitudes of asymmetry found for these increments, and equality of the gage readings is not a sufficient condition to assure uniform loading along the specimen.

Because of this asymmetry, the changes of specimen thickness at the two lower points of clip gage contact were unequal and the clip gage properly exhibited inclined fringes. The fringe orders in the clip gage and those in the specimen are equal at each of the gage contact points.

While the changes of thickness reveal severe asymmetry, the peak values of thickness changes near opposite sides of the hole boundary are nearly equal.

1/2 Inch Hole

Similar characteristics were observed for the 1/2 inch hole, except the patterns remained reasonably symmetrical in this case.

An unfortunate mistake for the first load increment resulted in no holographic exposure on one side of the specimen. The thickness change was not determined experimentally for the first increment. Instead, it was assumed to be equal to the thickness change measured for the second load increment--16,000 to 31,000 pounds.

1/4 Inch Hole

This specimen exhibited a very large degree of out-of-plane warpage, which increased progressively with applied load. When an object was viewed in the mirrorized portion of the specimen, it acted like a circus mirror that

grossly distorts the image. The specimen appeared to be curved in a shallow S-shape along the vertical axis and a shallow arc along the horizontal axis. Nevertheless, it sustained the predicted load.

The clip gage on this specimen became misaligned before the test when the load was adjusted to equalize the strain gage readings. In addition, the inclined fringes in the central vertical portion of the gage indicate that one lower leg of the gage separated from the specimen. It is presumed that this was caused by contact of the spring wire with the holographic plate as the specimen became severely warped.

The clip gage could still provide absolute fringe orders if one pair of (nominally) opposing legs remained in contact with the specimen. Of course, this would be on the side of the clip gage that exhibits lower fringe order, since the gap between specimen and gage leg would increase the fringe order on the opposite side. The fringe orders were interpreted with this assumption of clip gage behavior and the results appear to be entirely reasonable.

The changes of specimen thickness were nearly symmetrical until near the failure load. Failure did not occur along the central cross-section as in the other tests, but instead it failed near the upper grip in what has been described as a strain concentration anomaly.[4]

A remarkable quality of the optical method is illustrated dramatically in this test. The specimen was severely warped, and the two holograms sensed the severe warpage on each side of the specimen. The final pattern, however, revealed the algebraic sum of the warpages uniquely (i.e., it revealed the change of thickness alone), without regard to the magnitude of the general specimen warpage. It is this large warpage, however, that is responsible for the increased noise in the last few patterns in this sequence.

17

A curious and unexplained result is the much lower magnitudes of thickness changes occurring in this specimen compared to the other two. One is tempted to suppose that the clip gage did not give a reliable indication of the absolute fringe orders and presume that the fringe orders are higher than those shown here. However, the assignment of fringe orders as shown, assuming reliable data from the clip gage, places the zero-order fringe in the right location. This location is consistent with the other tests and consistent with reasonable expectations. If the fringe order remote from the hole is assumed to be much higher than shown, the zero-order fringe would not be consistent with results of the other specimens.

The specimen with the 1/4 inch hole was not from the same batch of material as the other two. Of the three specimens received for these tests, the one with the 1/4 inch hole was found to be defective in the C-scan tests. It was put aside in favor of a similar specimen received earlier, which exhibited a superior C-scan appraisal. We do not know whether this is a factor in the thickness change performance of this specimen.

CONCLUSIONS

Contour maps of thickness changes were obtained for three quasi-isotropic graphite-epoxy plates with central holes, loaded in compression. For each specimen, thickness changes were determined for six load increments from nearly zero to within a few percent of the failure load. From these whole-field patterns, the cumulative thickness changes can be obtained in the entire field, and they are plotted for the horizontal centerline. The contour interval was 12.5 μin., or 12.5 μin. change of thickness occurred between neighboring contours.

A new optical technique was developed to obtain these whole-field maps of thickness change. It utilizes a comparatively simple means of holographic interferometry on both sides of the specimen, followed by additive moire to obtain thickness changes as the sum of the out-of-plane displacements.

REFERENCES

1. C. M. Vest, Holographic Interferometry, John Wiley & Sons, New York (1979).

2. D. B. Newmann and R. C. Penn, "Off-table Holography," Experimental Mechanics, 15(6), 241-244 (June 1975).

3. A. J. Durelli and V. J. Parks, Moire Analysis of Strain, Prentice-Hall, Inc., Englewood Cliffs, NJ (1970).

4. J. F. Knauss, J. H. Starnes, Jr., and E. G. Henneke, II, "The Compressive Failure of Graphite/Epoxy Plates with Circular Holes," VPI Report No. VPI-E-78-5 (February 1978).

TABLE I
Specimen with 3/4 inch hole

Preliminary adjustment of load axiality was performed at 10000 lbs

Hologram Pair No. I   Initial Load - 1050 lbs   Clock Time - 12:20

Exposure[a]	Clock Time	Load(lbs)	Strain Gage Readings[b]			
			RF	RR	LF	LR
1	12:43	1050	18	17	8	5
2	12:51	15950	163	162	169	170

Hologram Pair No. II   Initial Load - 16000 lbs   Clock Time - 12:46

Exposure	Clock Time	Load(lbs)	Strain Gage Readings			
			RF	RR	LF	LR
1	1:03	15900	163	161	168	170
2	1:11	30700	313	304	334	333

Hologram Pair No. III   Initial Load - 31000 lbs   Clock Time - 1:06

Exposure	Clock Time	Load(lbs)	Strain Gage Readings			
			RF	RR	LF	LR
1	1:21	30600	313	303	334	332
2	1:30	45850	467	449	515	511

Hologram Pair No. IV   Initial Load - 46000 lbs   Clock Time - 1:25

Exposure	Clock Time	Load(lbs)	Strain Gage Readings			
			RF	RR	LF	LR
1	1:42	45700	467	448	515	510
2	1:50	53850	545	521	620	613

Hologram Pair No. V   Initial Load - 54000 lbs   Clock Time - 1:45

Exposure	Clock Time	Load(lbs)	Strain Gage Readings			
			RF	RR	LF	LR
1	2:04	53700	545	521	619	612
2	2:12	56750	573	547	662	653

Hologram Pair No. VI   Initial Load -57000 lbs   Clock Time - 2:07

Exposure	Clock Time	Load(lbs)	Strain Gage Readings			
			RF	RR	LF	LR
1	2:25	56650	573	547	662	653
2	2:33	59750	601	575	705	695

Initial Load - 60000 lbs   Clock Time - 2:28

	Clock Time	Load(lbs)	Strain Gage Readings			
			RF	RR	LF	LR
	2:41	52000	622	594	735	723

Failure Load - 64000 lbs

(a)   The inclination of the photographic plates is adjusted before and after each
      exposure by +θ and -θ respectively.
(b)   These readings are of axial strain corresponding to a reduction in length.
      RF - right front, RR - right rear, LF - left front, LR - left rear.

20

TABLE II
Specimen with 1/2 inch hole

Preliminary adjustment of load axiality was performed at 15000 lbs

Hologram Pair No. I   Initial Load - 1000 lbs   Clock Time - 1:26

Exposure[a]	Clock Time	Load(lbs)	Strain Gage Readings[b]			
			RF	RR	LF	LR
1	1:40	1000	17	12	7	10
2	1:49	15900	157	158	159	160

Hologram Pair No. II   Initial Load - 16000 lbs   Clock Time - 1:43

Exposure	Clock Time	Load(lbs)	Strain Gage Readings			
			RF	RR	LF	LR
1	1:59	15900	156	158	158	159
2	2:12	30700	309	305	320	317

Hologram Pair No. III   Initial Load - 31000 lbs   Clock Time - 2:07

Exposure	Clock Time	Load(lbs)	Strain Gage Readings			
			RF	RR	LF	LR
1	2:26	30650	307	303	319	316
2	2:35	45800	461	454	490	485

Hologram Pair No. IV   Initial Load - 46000 lbs   Clock Time - 2:29

Exposure	Clock Time	Load(lbs)	Strain Gage Readings			
			RF	RR	LF	LR
1	2:50	45650	461	453	490	483
2	2:57	60600	607	595	620	667

Hologram Pair No. V   Initial Load - 61000 lbs   Clock Time - 2:52

Exposure	Clock Time	Load(lbs)	Strain Gage Readings			
			RF	RR	LF	LR
1	3:14	60400	606	594	678	666
2	3:22	64700	646	632	739	724

Hologram Pair No. VI   Initial Load - 65000 lbs   Clock Time - 3:16

Exposure	Clock Time	Load(lbs)	Strain Gage Readings			
			RF	RR	LF	LR
1	3:39	64600	645	631	739	724
2	3:47	67650	671	657	784	766

Initial Load - 68000 lbs   Clock Time - 3:41

Failed at 72600 lbs

(a)   The inclination of the photographic plates is adjusted before and after each exposure by $+\theta$ and $-\theta$ respectively.

(b)   These readings are of axial strain corresponding to a reduction in length. RF - right front, RR - right rear, LF - left front, LR - left rear.

TABLE III
Specimen with 1/4 inch hole

Preliminary adjustment of load axiality was performed at 15000 lbs

<u>Hologram Pair No. I</u>　　　　　Initial Load - 1100 lbs　　　Clock Time - 11:15

Exposure[a]	Clock Time	Load(lbs)	Strain Gage Readings[b]			
			RF	RR	LF	LR
1	11:24	1100	11	11	12	10
2	11:33	15850	123	126	123	123

<u>Hologram Pair No. II</u>　　　　Initial Load - 16000 lbs　　　Clock Time - 11:27

Exposure	Clock Time	Load(lbs)	Strain Gage Readings			
			RF	RR	LF	LR
1	11:44	15750	123	125	123	122
2	11:53	30800	251	249	233	233

<u>Hologram Pair No. III</u>　　　　Initial Load - 31000 lbs　　　Clock Time - 11:47

Exposure	Clock Time	Load(lbs)	Strain Gage Readings			
			RF	RR	LF	LR
1	1:12	30500	250	247	231	231
2	1:20	45800	390	381	336	338

<u>Hologram Pair No. IV</u>　　　　Initial Load - 46000 lbs　　　Clock Time - 1:14

Exposure	Clock Time	Load(lbs)	Strain Gage Readings			
			RF	RR	LF	LR
1	1:31	45650	390	384	336	337
2	1:40	60850	536	533	412	433

<u>Hologram Pair No. V</u>　　　　Initial Load - 61000 lbs　　　Clock Time - 1:34

Exposure	Clock Time	Load(lbs)	Strain Gage Readings			
			RF	RR	LF	LR
1	1:52	60700	536	532	411	432
2	2:00	70600	638	649	436	483

Plate had buckled appearance

<u>Hologram Pair No. VI</u>　　　　Initial Load - 71000 lbs　　　Clock Time - 1:54

Exposure	Clock Time	Load(lbs)	Strain Gage Readings			
			RF	RR	LF	LR
1	2:28	70300	637	650	433	481
2	2:37	73800	688	706	432	489

Initial Load - 74000 lbs　　　Clock Time - 2:31

Failed at 78000 lbs

---

[a]　The inclination of the photographic plates is adjusted before and after each exposure by $+\theta$ and $-\theta$ respectively.

[b]　These readings are of axial strain corresponding to a reduction in length. RF - right front, RR - right rear, LF - left front, LR - left rear.

Spec.	Hole dia. A (in.)	Thickness (in.)
1	3/4	0.265
2	1/2	0.267
3	1/4	0.264
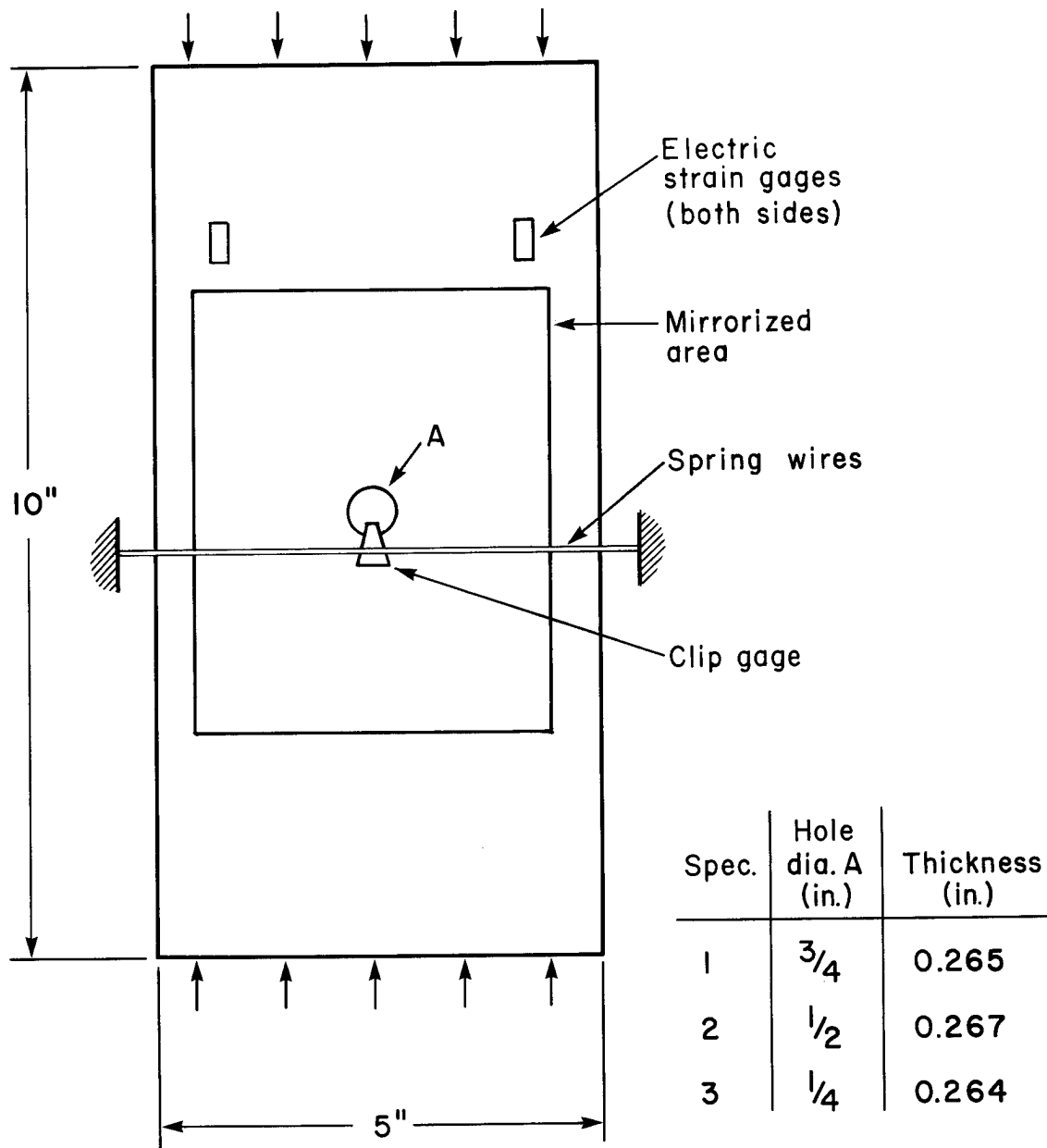
Fig. 1. Graphite-epoxy composite specimens for compression tests.

$$\Delta T = W_{I} + W_{II}$$
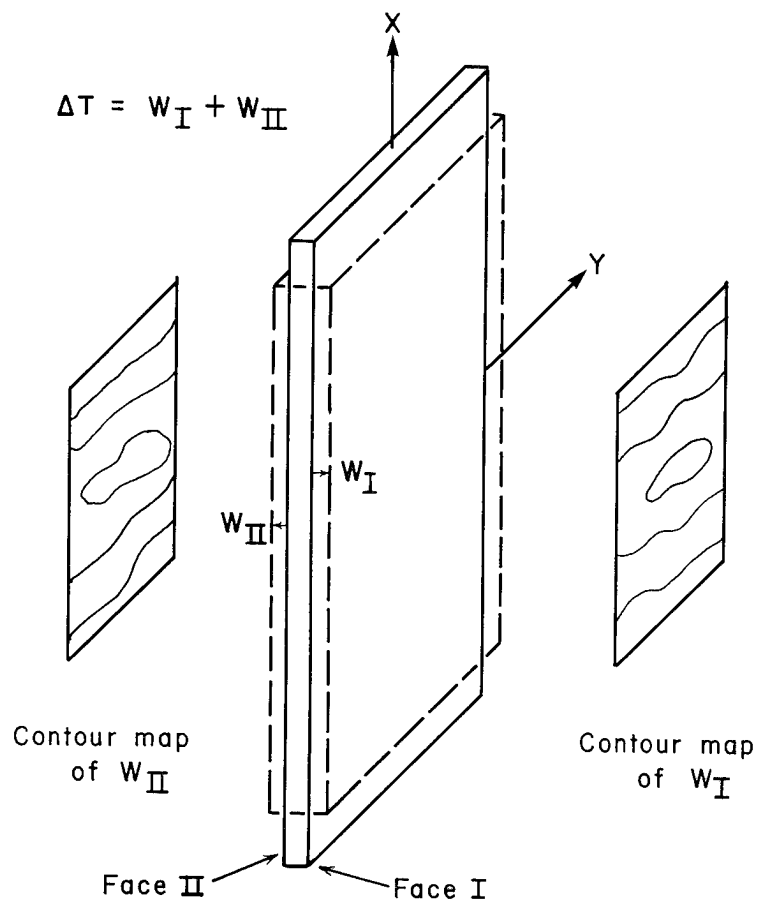
Fig. 2. Out-of-plane displacements of specimen surfaces, shown greatly exaggerated.
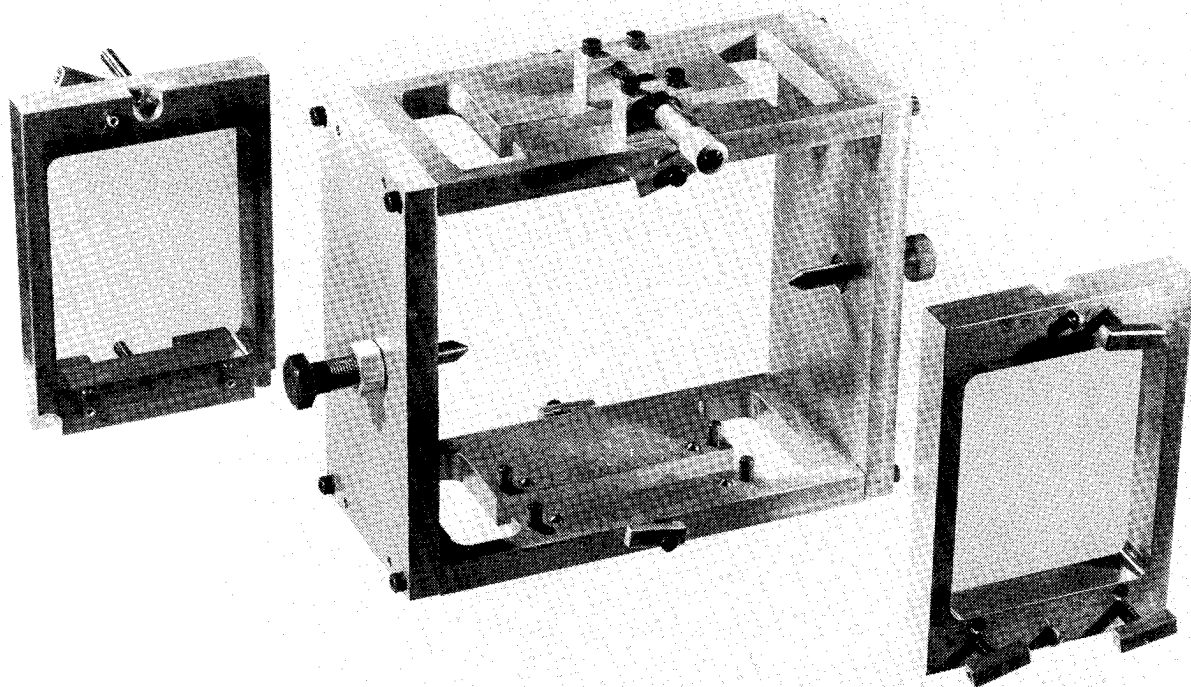
Fig. 3. Fixture for Reflection Holography. The box-like fixture attaches to
the specimen and pivots about its y-axis; the micrometer adjusts inclination
of the fixture. Conical seats are cemented to the specimen to prevent damage
by the pivot points. Photographic plates are clipped onto each frame and
subsequently inserted into the fixture.
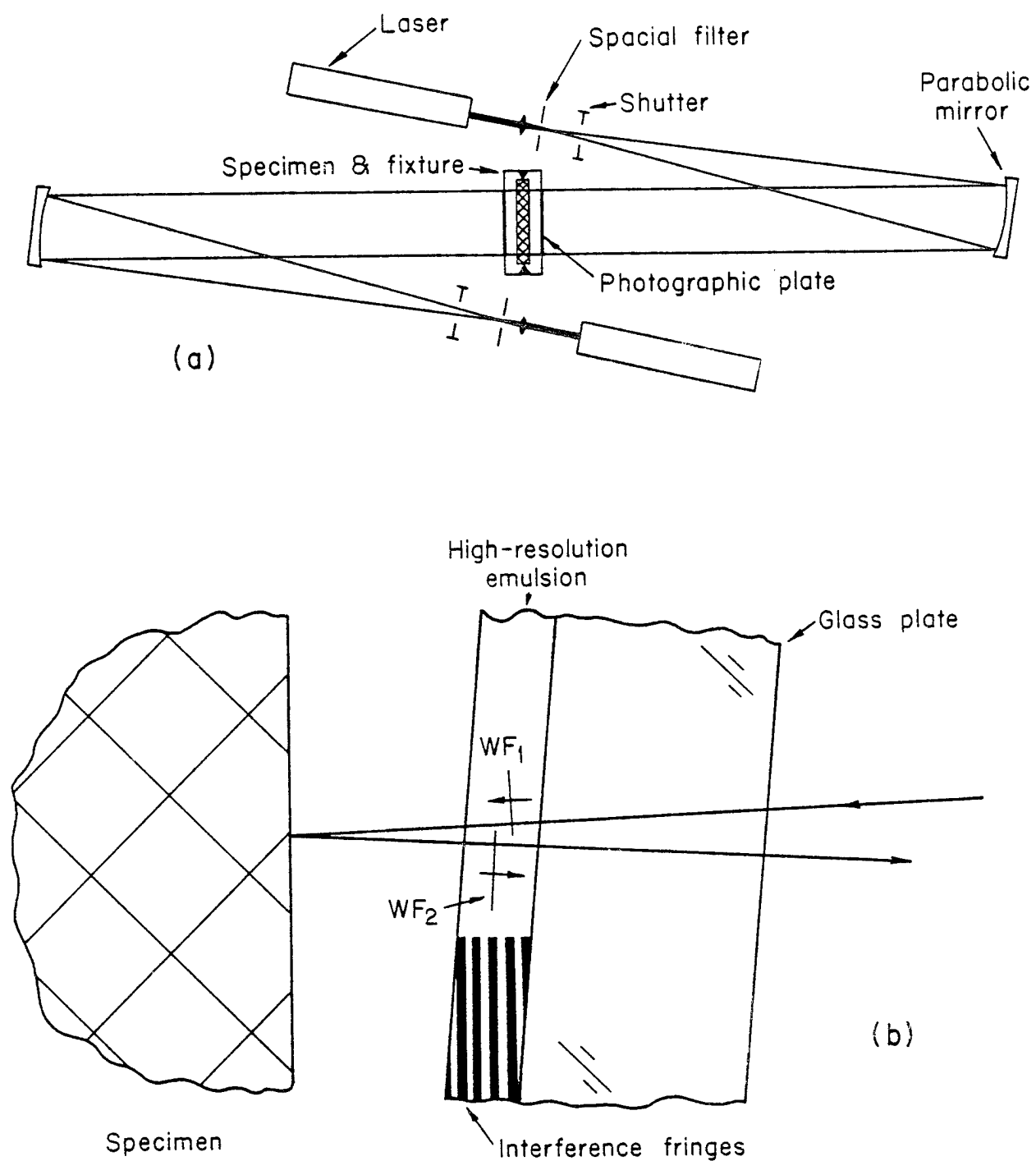
Fig. 4. (a) Optical system for the holographic exposures. (b) The incoming (reference) beam and reflected (information) beam form a stationary pattern of constructive and destructive interference in the volume of the photographic emulsion.

Emulsion

Glass plate

B ——————— B

A ——————— A

Center planes of walls of
constructive interference
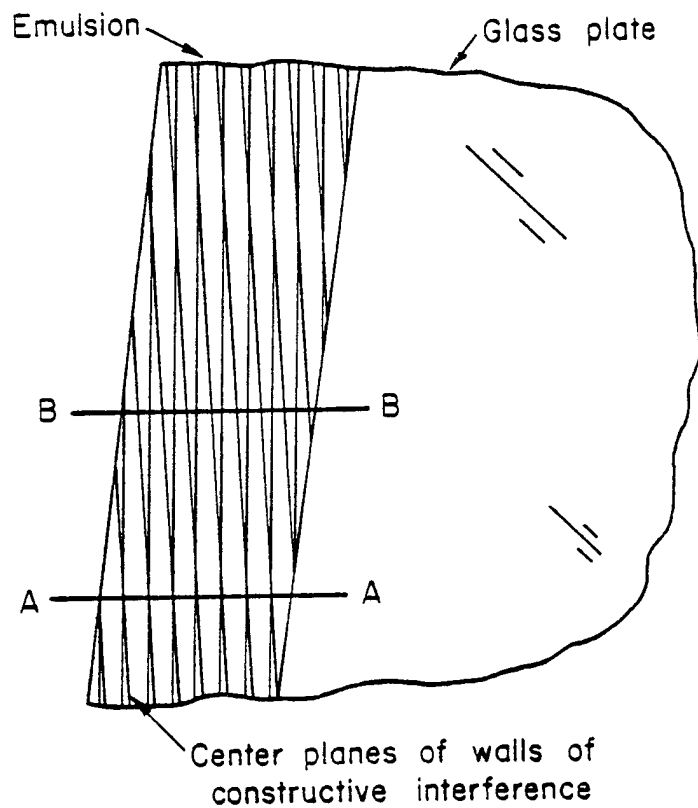
Fig. 5. Each doubly-exposed
photographic plate captures
two systems of interference
fringes, representing specimen
surface warpage before and
after the load increment,
respectively.

From exposure 1

From exposure 2

From interface
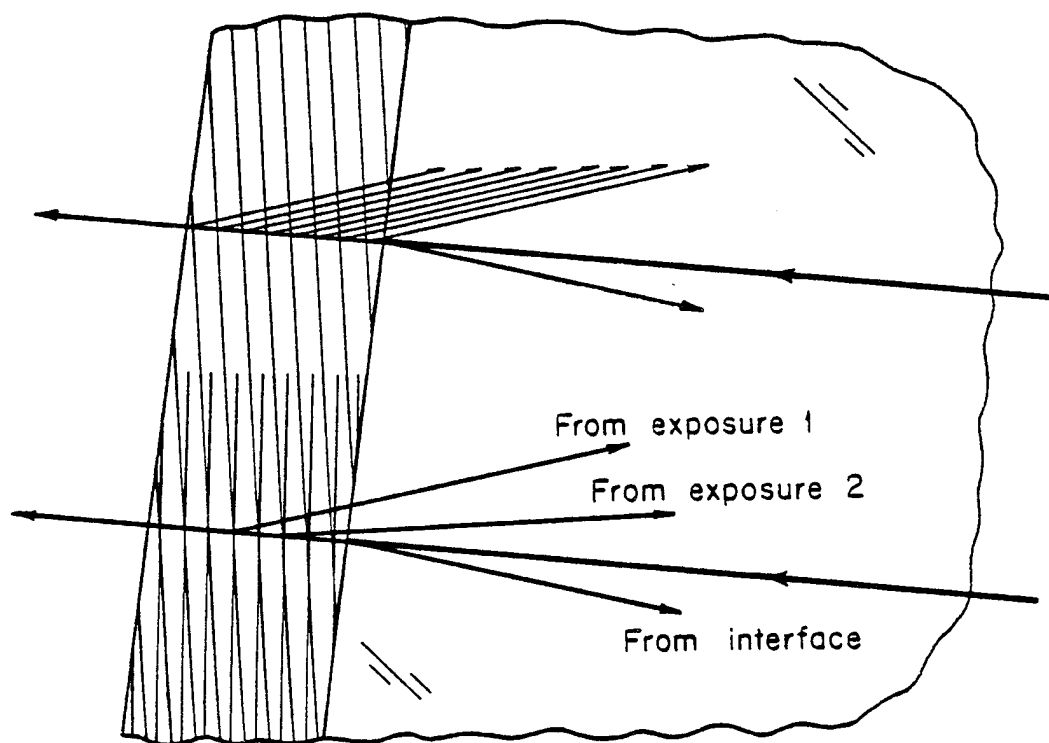
Fig. 6. After development, the walls of constructive interference become
partial mirrors and reflect light in the direction taken by the information
beam at the time of the holographic exposure.

27
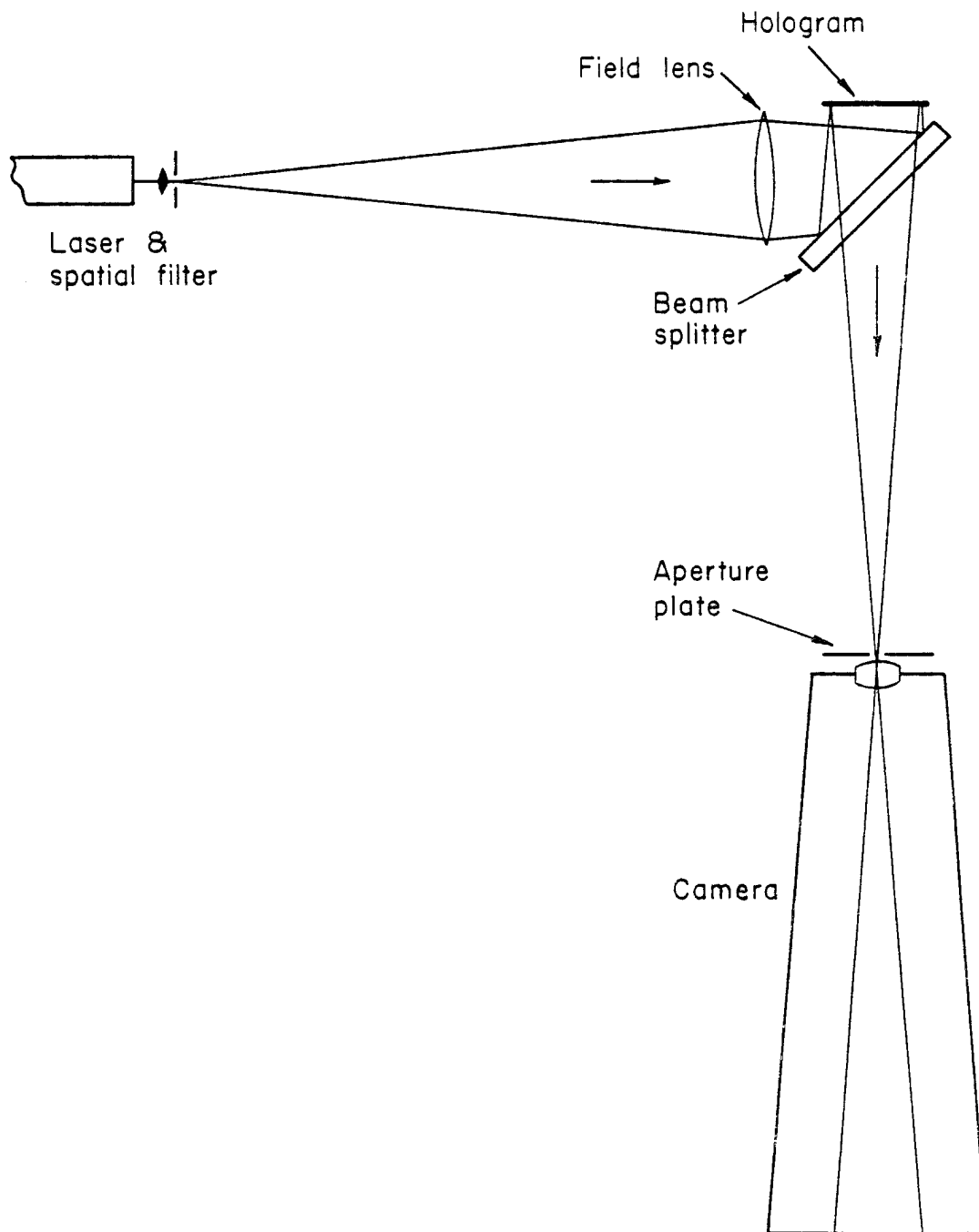
Fig. 7. Optical system used to reconstruct the hologram images.
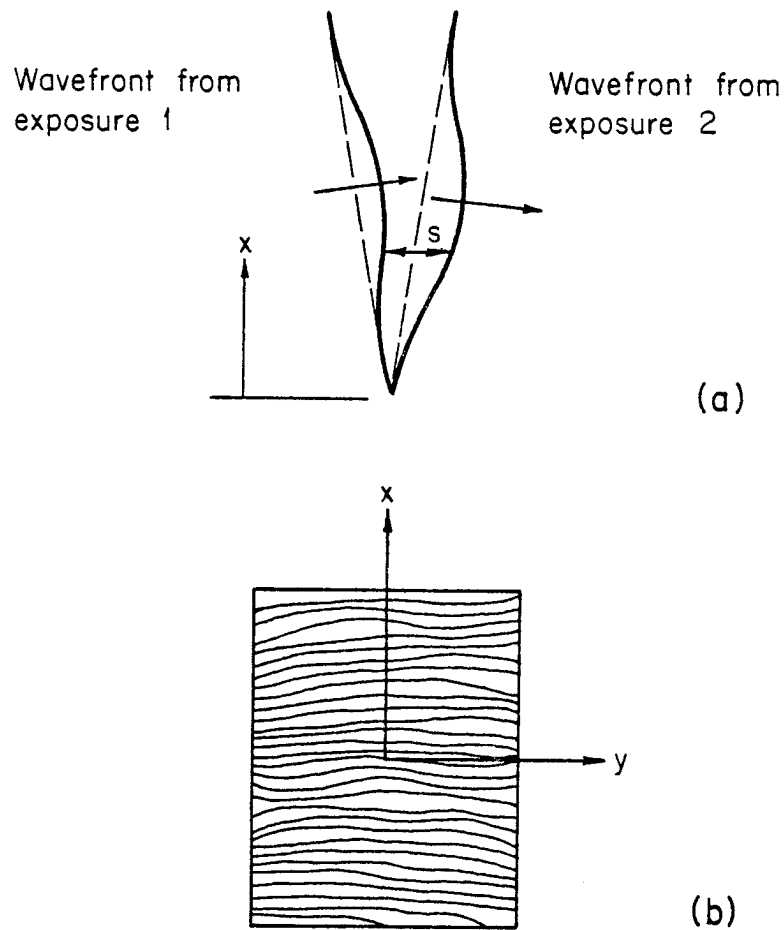
Fig. 8.   (a) Upon reconstruction, wavefronts emerge from each hologram with warpage representing the specimen surface before and after the load increment; their relative inclination forms a carrier pattern. (b) They combine through optical interference to form a contour map of s, where information depicting the difference of wavefront warpages appears as disturbances in the otherwise regular carrier pattern.

$N_y =$

(a)

(b)

Laser

Two superimposed films

Aperture plate

Diffraction orders
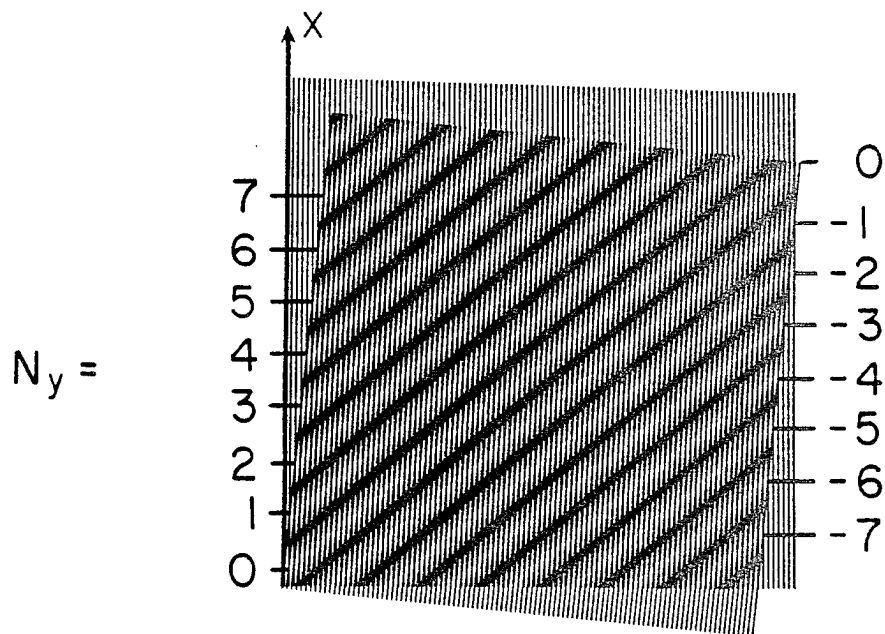
Camera
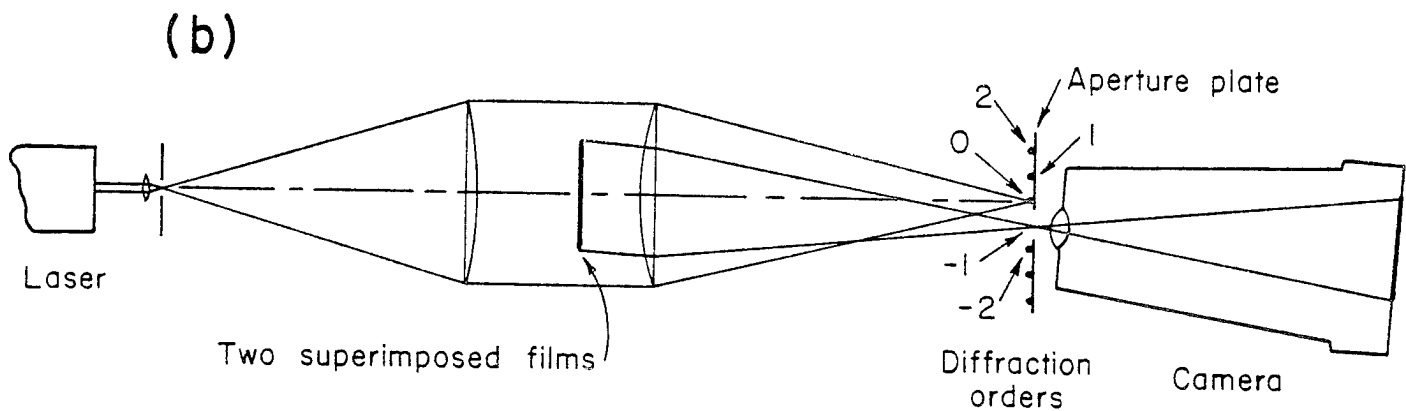
Fig. 9. (a) Superposition of the contour maps from faces I and II forms moire fringes that depict changes of specimen thickness. (b) Arrangement for optical filtering to enhance contrast of the moire fringes.
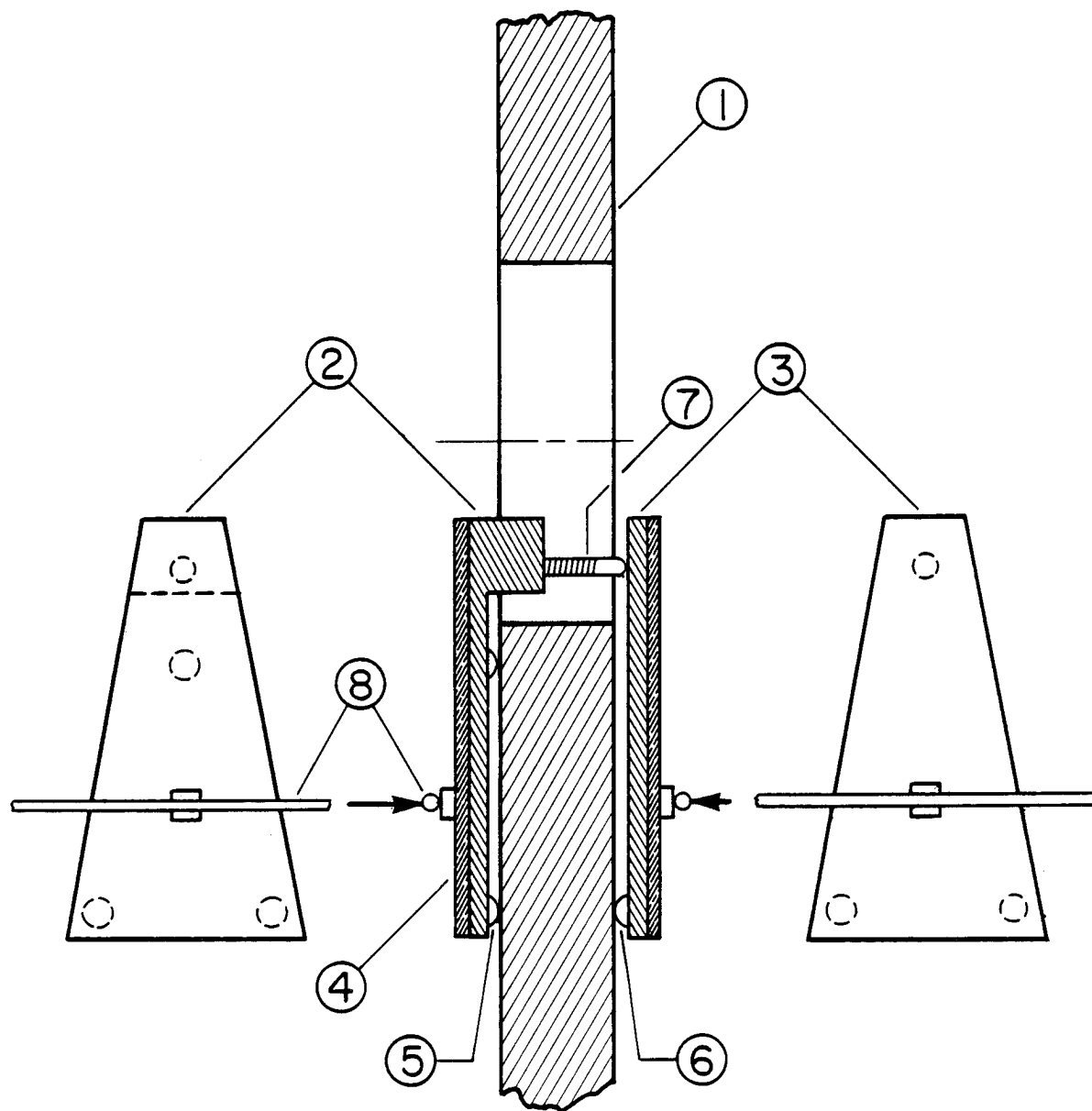
① specimen   ⑤ 3 legs contact specimen

② plate I   ⑥ 2 legs contact specimen

③ plate II   ⑦ adjustable contact for plate II

④ aluminumized glass   ⑧ spring wires

Fig. 10. Configuration and location of Clip Gage 2 used to measure the absolute change of thickness at a point in the field of view.
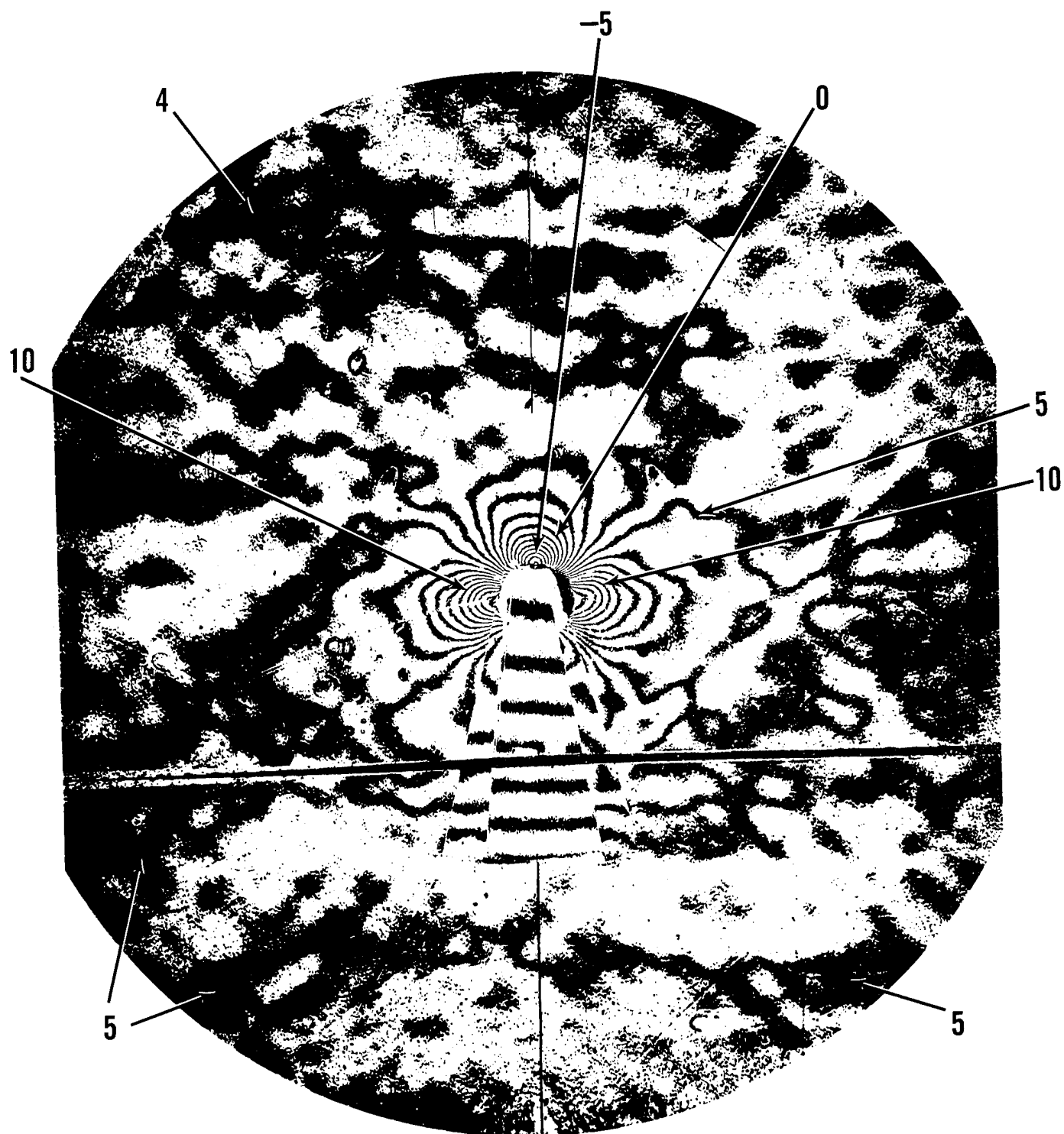
31
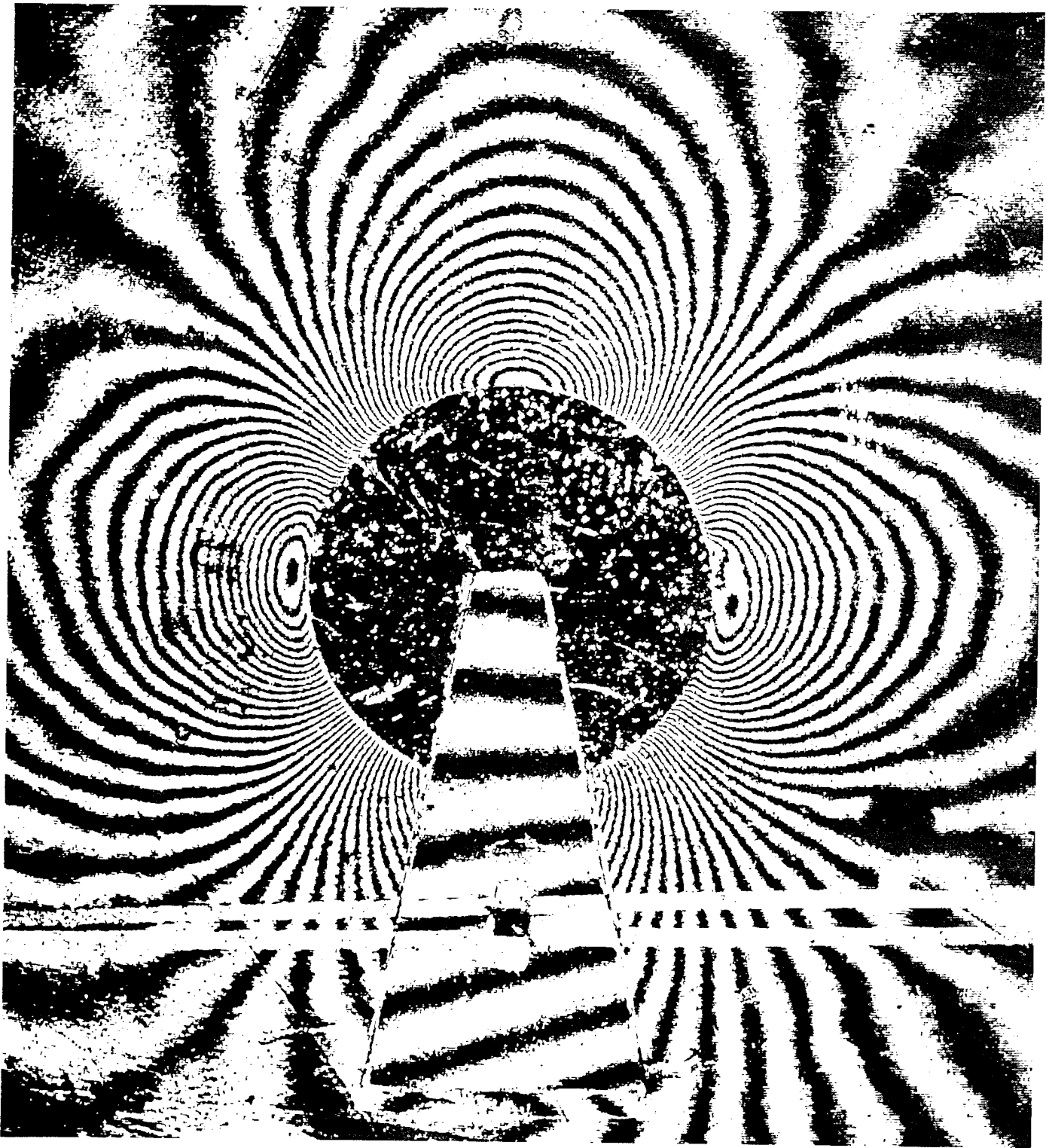
Fig. 11. Change of thickness contour maps for the test specimen containing a 3/4 inch hole. (a) Load increment no. 1; 1,000 - 16,000 pounds; enlarged view of center portion.
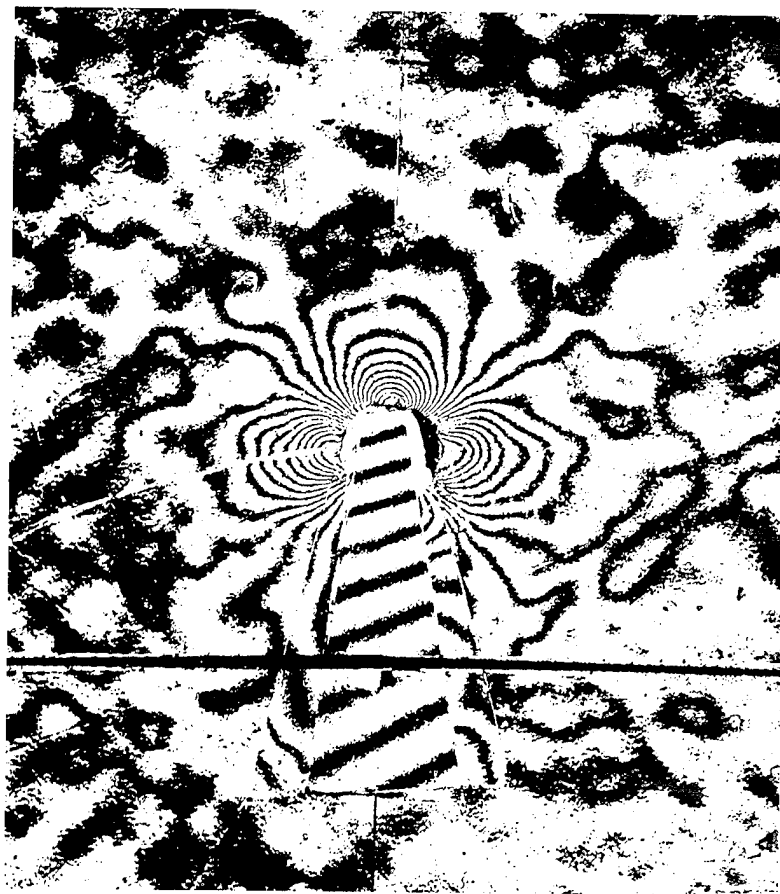
Fig. 11(b). Load increment no. I; 1,000 - 16,000 pounds; 3/4" hole.
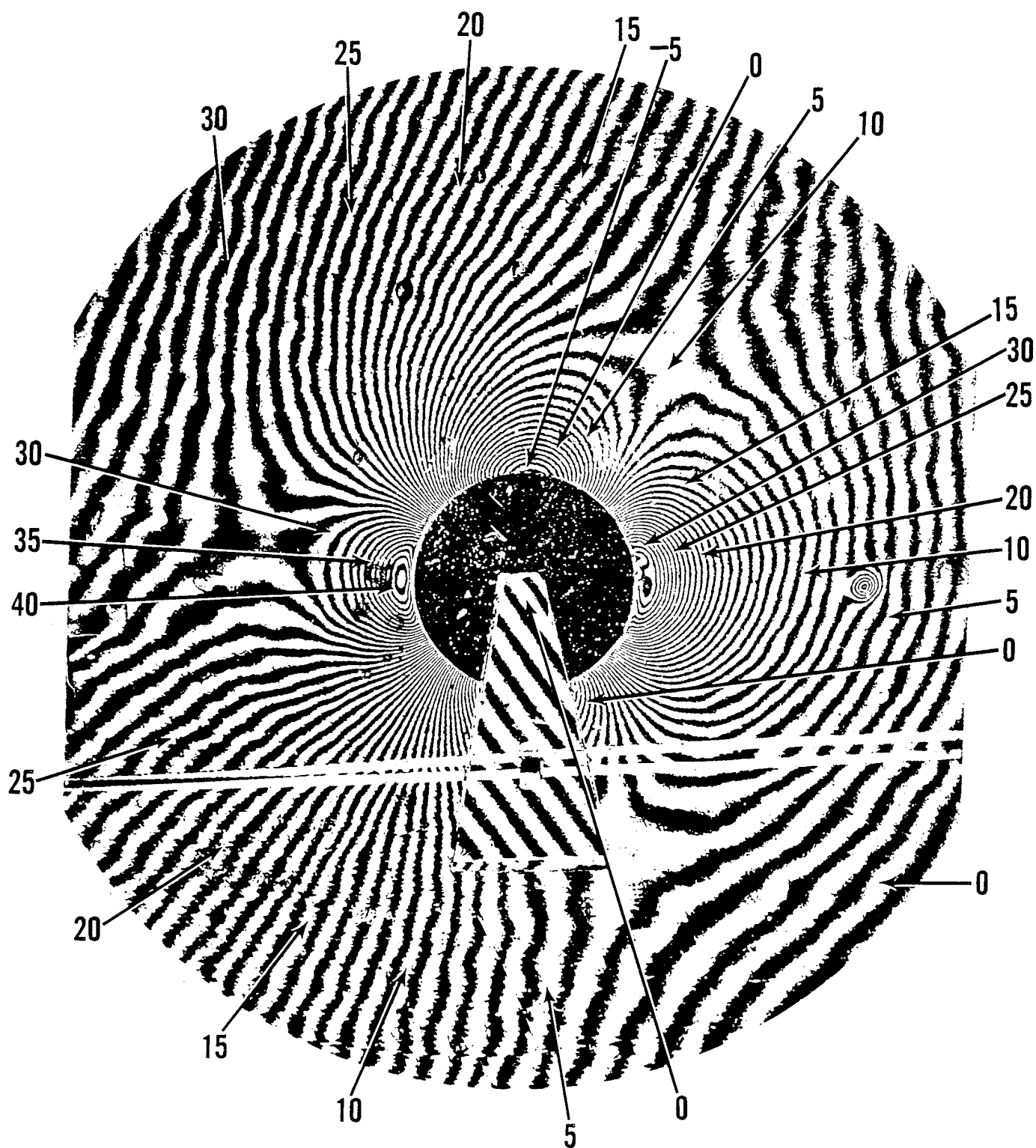
Fig. 11(c). Load increment no. II; 16,000 - 31,000 pounds; 3/4" hole.

34
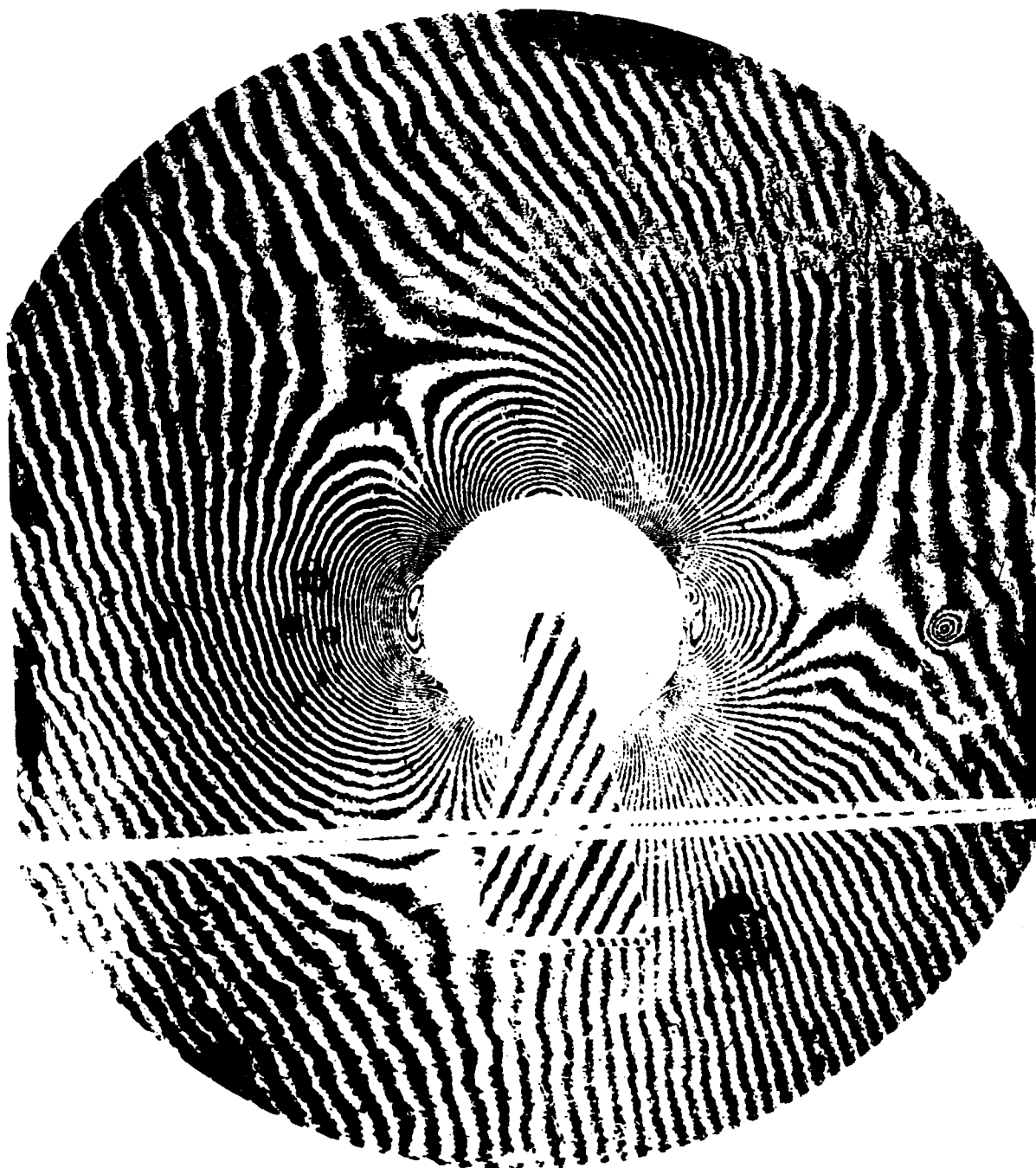
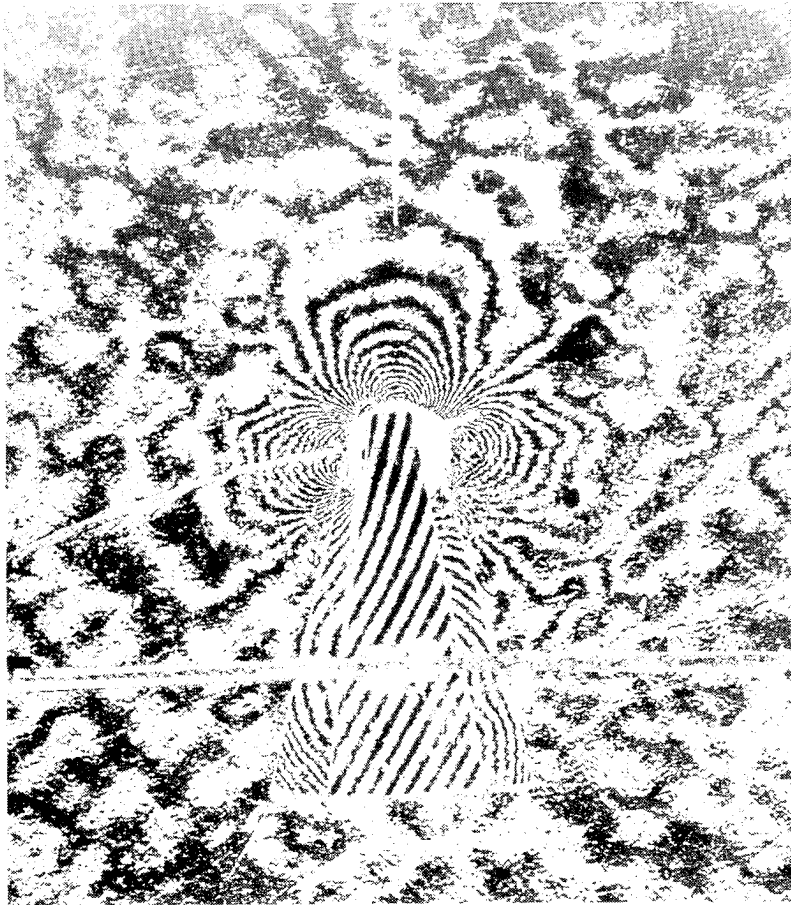Fig. 11(d). Load increment no. III; 31,000 - 46,000 pounds; 3/4" hole.
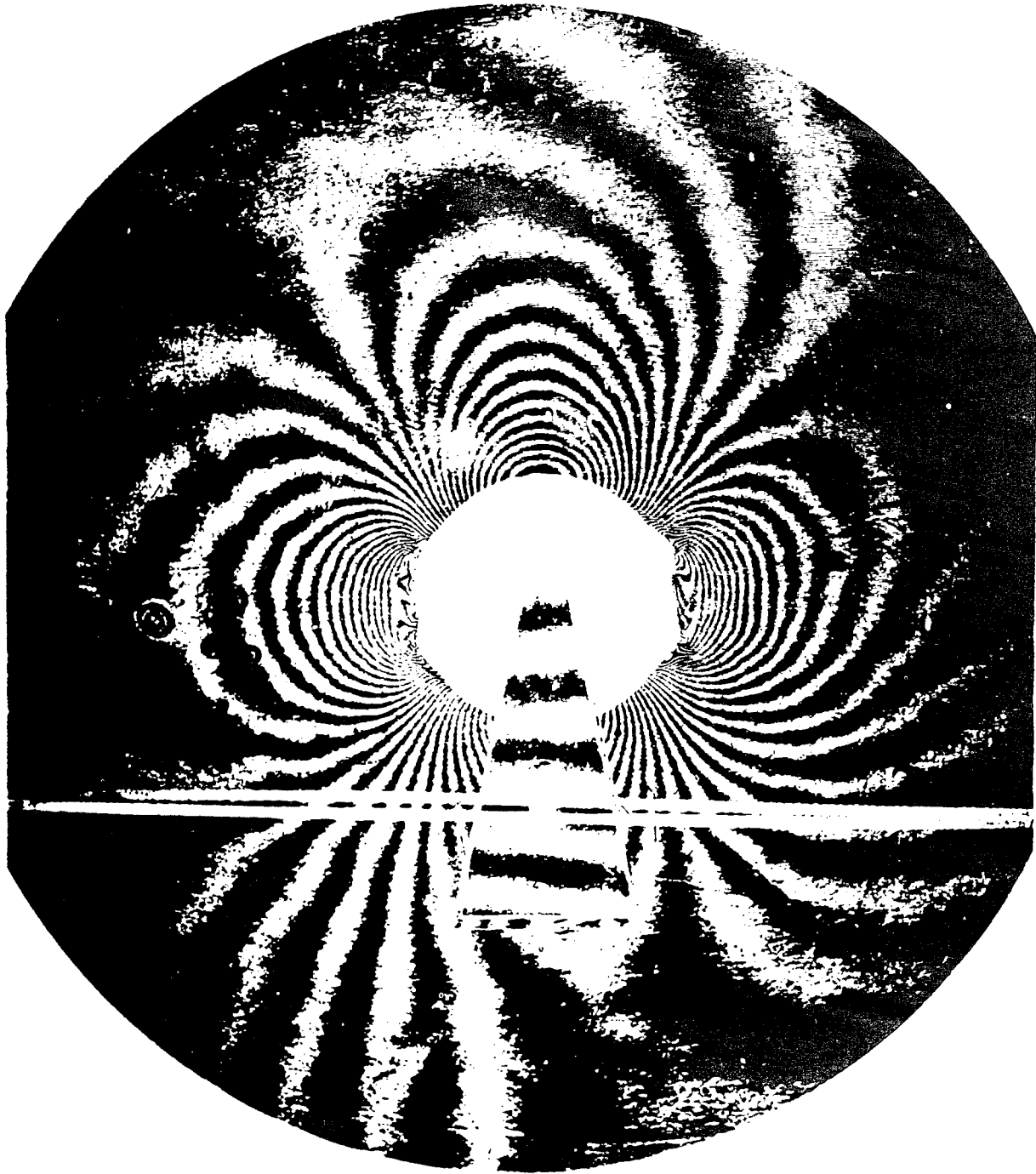
Fig. 11(e). Load increment no. IV; 46,000 - 54,000 pounds; 3/4" hole.
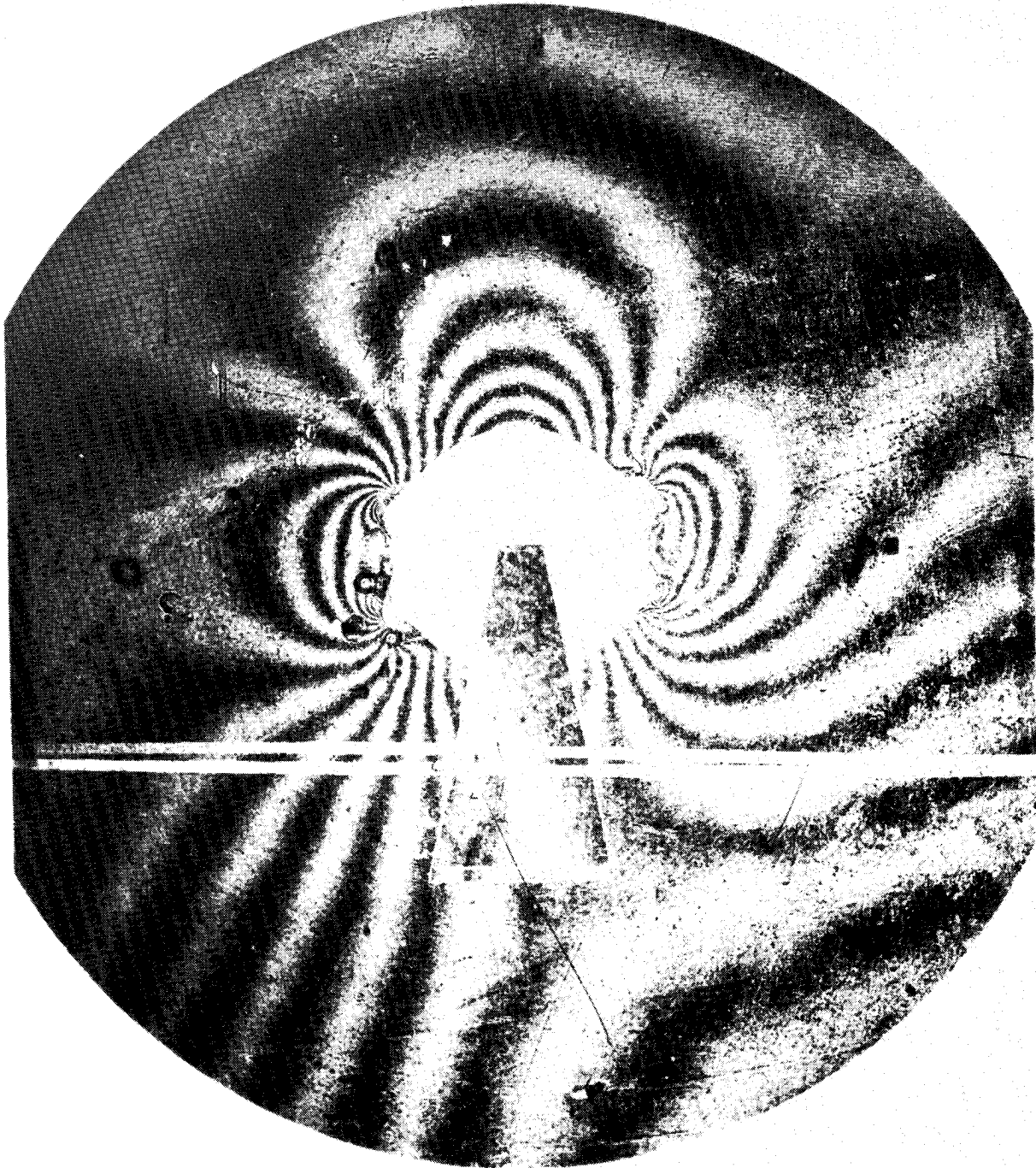
Fig. 11(f). Load increment no. V; 54,000 - 57,000 pounds; 3/4" hole.
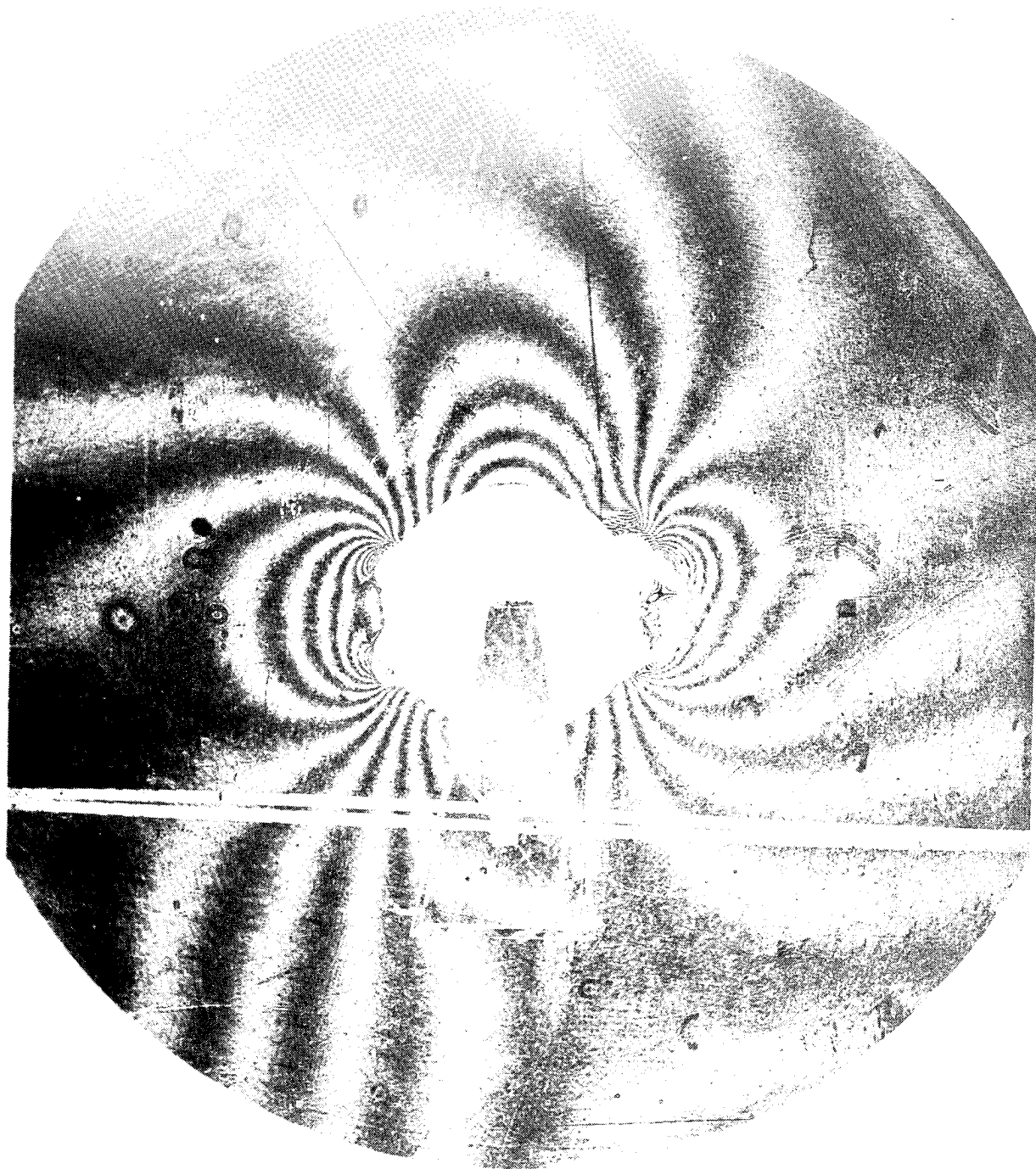
Fig. 11(g). Load increment no. VI; 57,000 - 60,000 pounds; 3/4" hole.
(Failure load 64,000 pounds.)
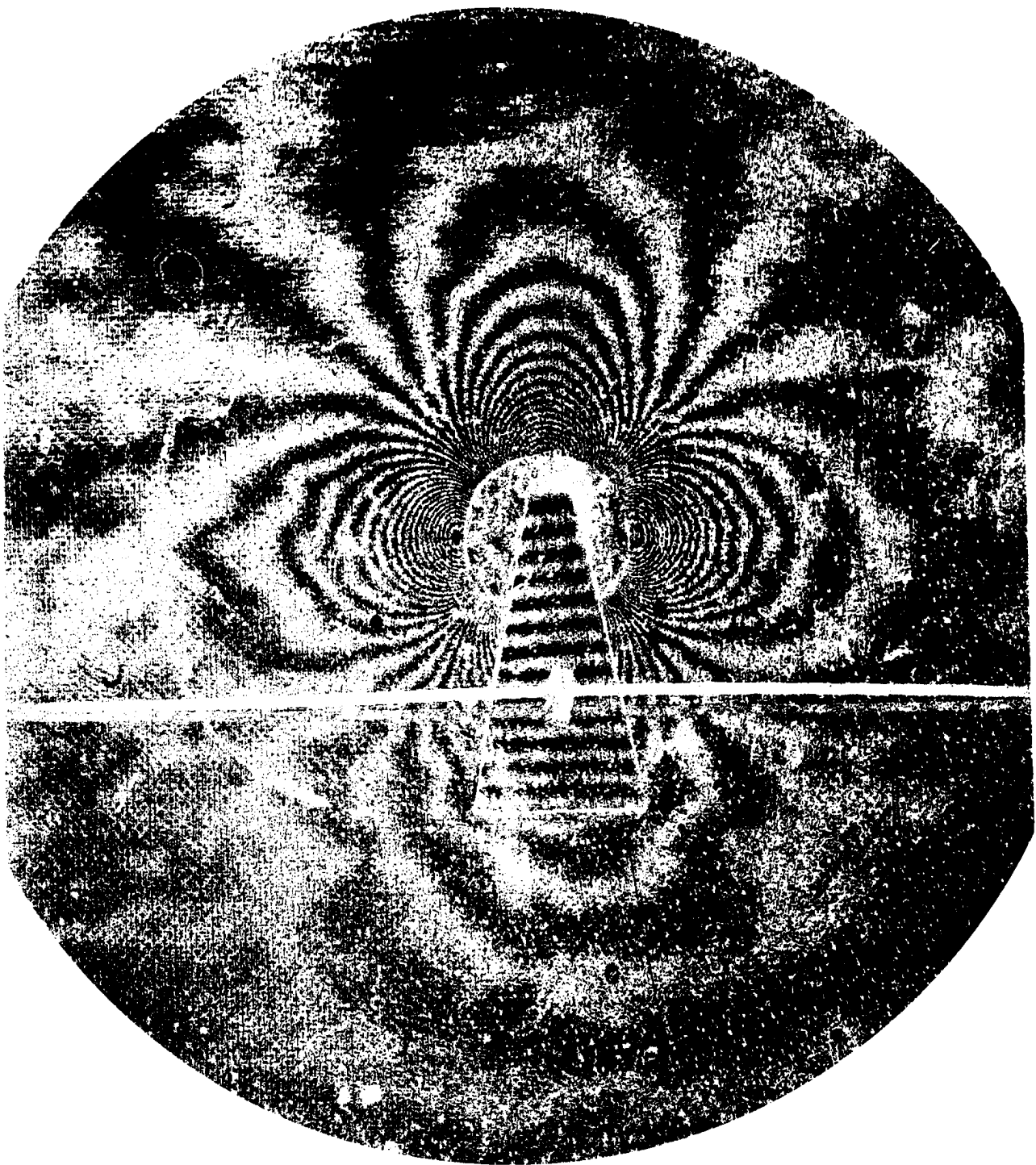
Fig. 12. Change of thickness contour maps for the test specimen containing a 1/2 inch hole. 12(a). Load increment no. II; 16,000 - 31,000 pounds; 1/2" hole.

Fig. 12(b). Load increment no. III; 31,000 - 46,000 pounds; 1/2" hole.
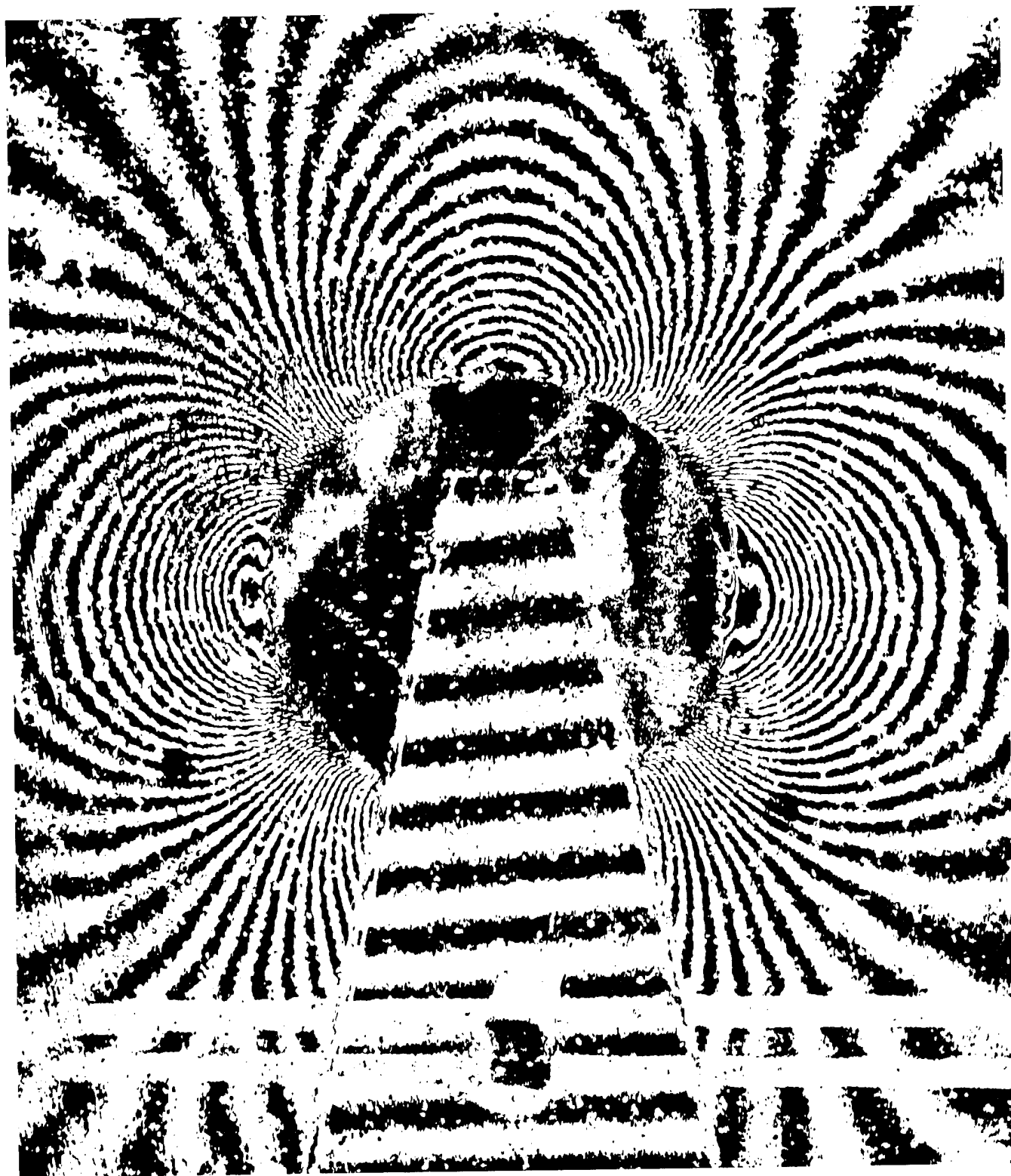
Fig. 12(c). Load increment no. III; 31,000 - 46,000 pounds; 1/2" hole; enlarged view of center portion.

Fig. 12(d). Load increment no. IV; 46,000 - 61,000 pounds; 1/2" hole.

Fig. 12(e). Load increment no. V; 61,000 - 65,000 pounds; 1/2" hole.
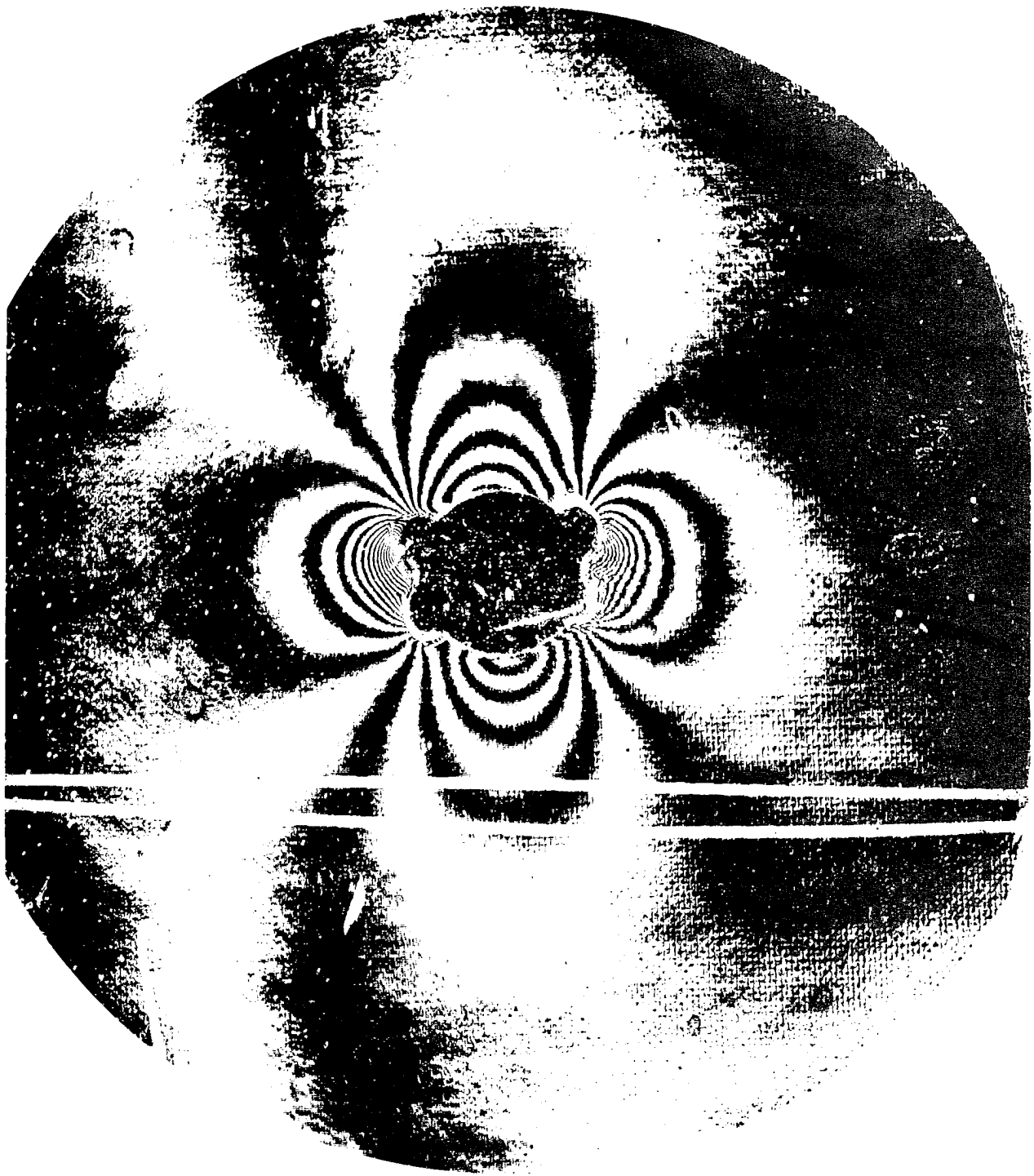
Fig. 12(f). Load increment no. VI; 65,000 - 67,000 pounds; 1/2" hole.
(Failure load 72,000 pounds.)

Fig. 13. Change of thickness contour maps for the test specimen containing a 1/4 inch hole. (a). Load increment no. l; 1,000 - 16,000 pounds; 1/4" hole.

45

Fig. 13(b). Load increment no. II; 16,000 - 31,000 pounds; 1/4" hole.
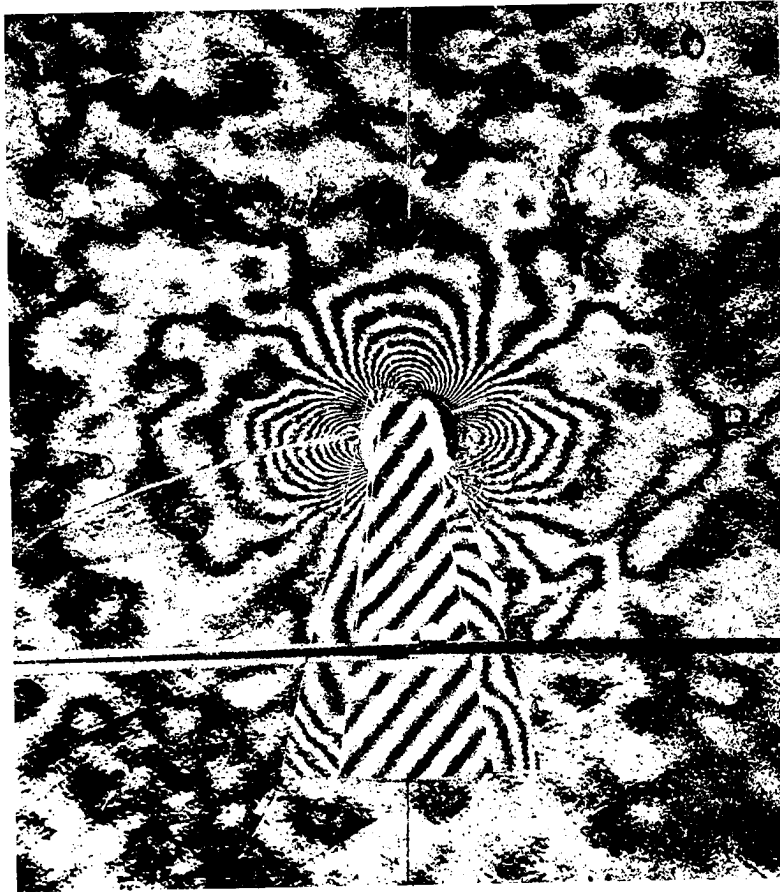
Fig. 13(c). Load increment no. III; 31,000 - 46,000 pounds; 1/4" hole.

Fig. 13(d). Load increment no. IV; 46,000 - 61,000 pounds; 1/4" hole.
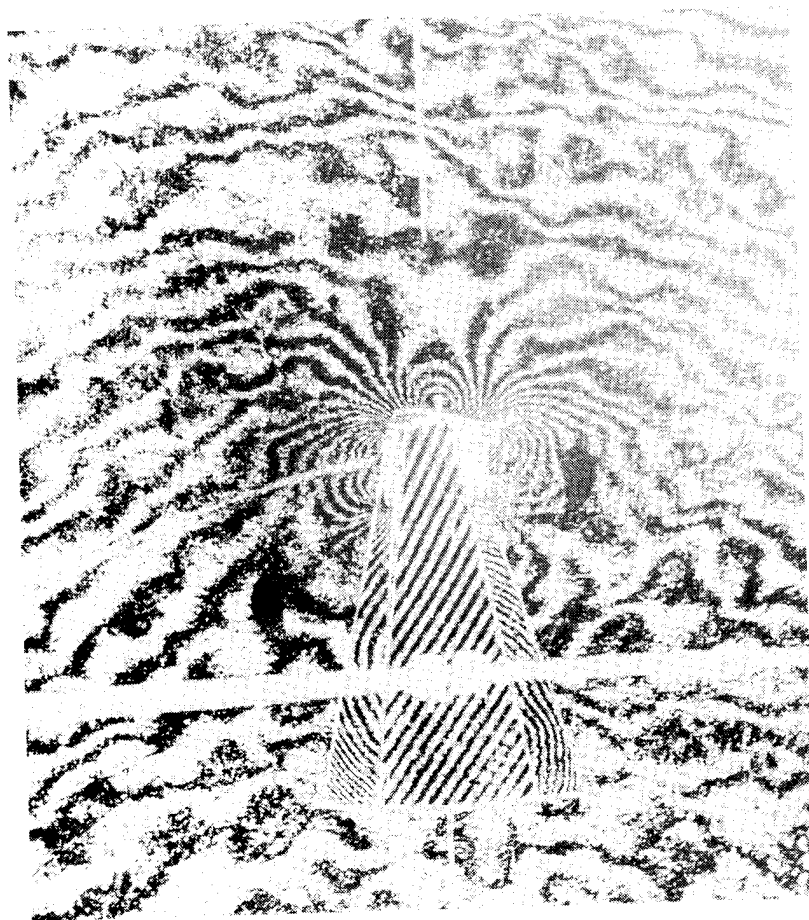
Fig. 13(e). Load increment no. V; 61,000 - 71,000 pounds; 1/4" hole.
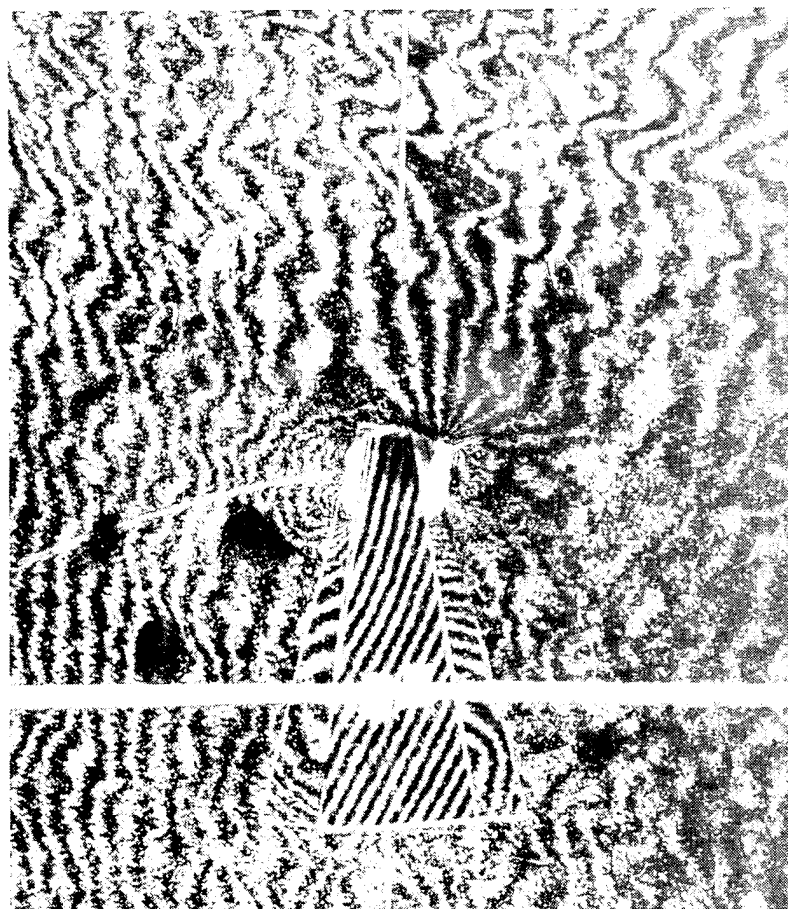
Fig. 13(f). Load increment no. VI; 71,000 - 74,000 pounds; 1/4" hole.
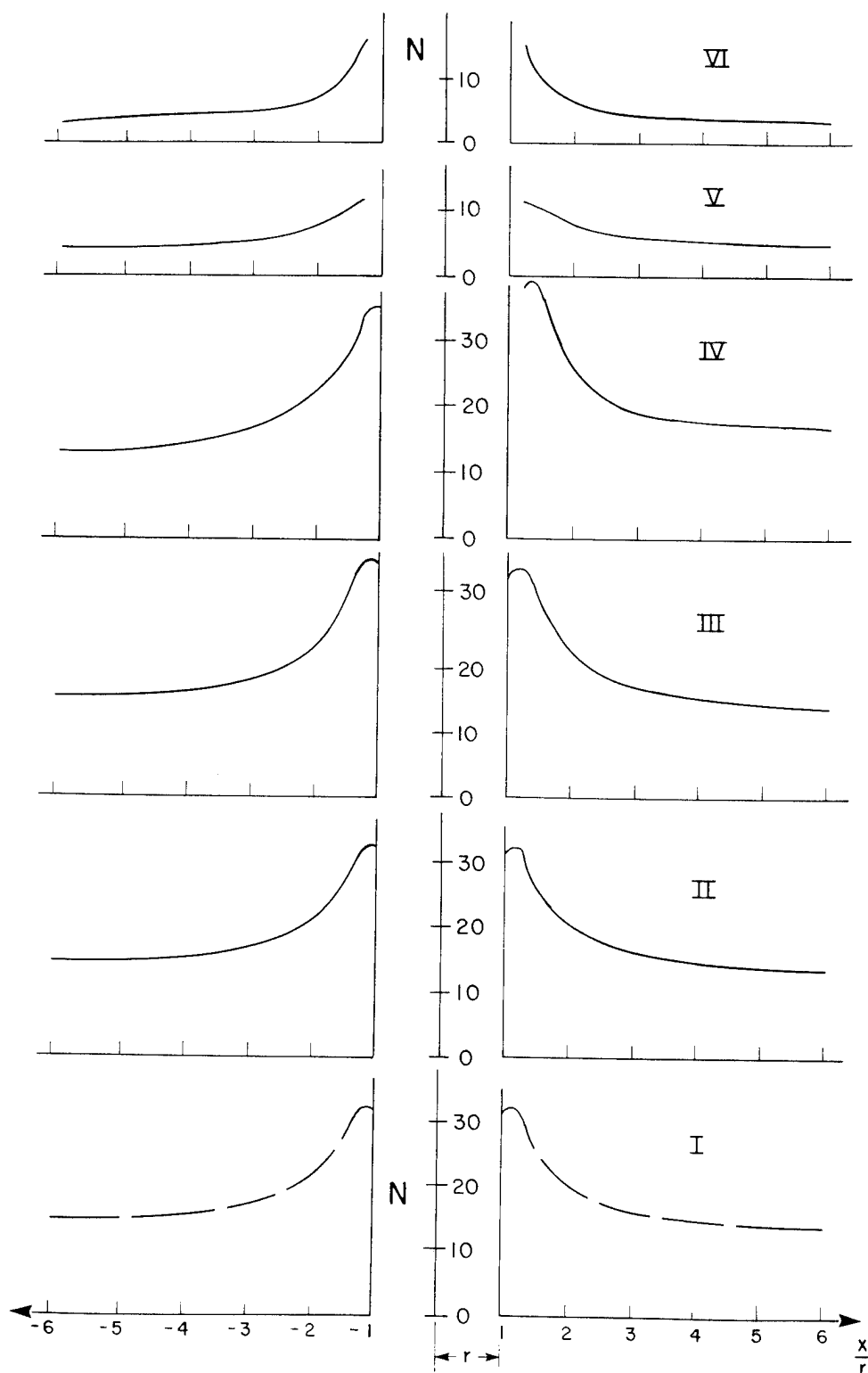(Failure load 78,000 pounds.)
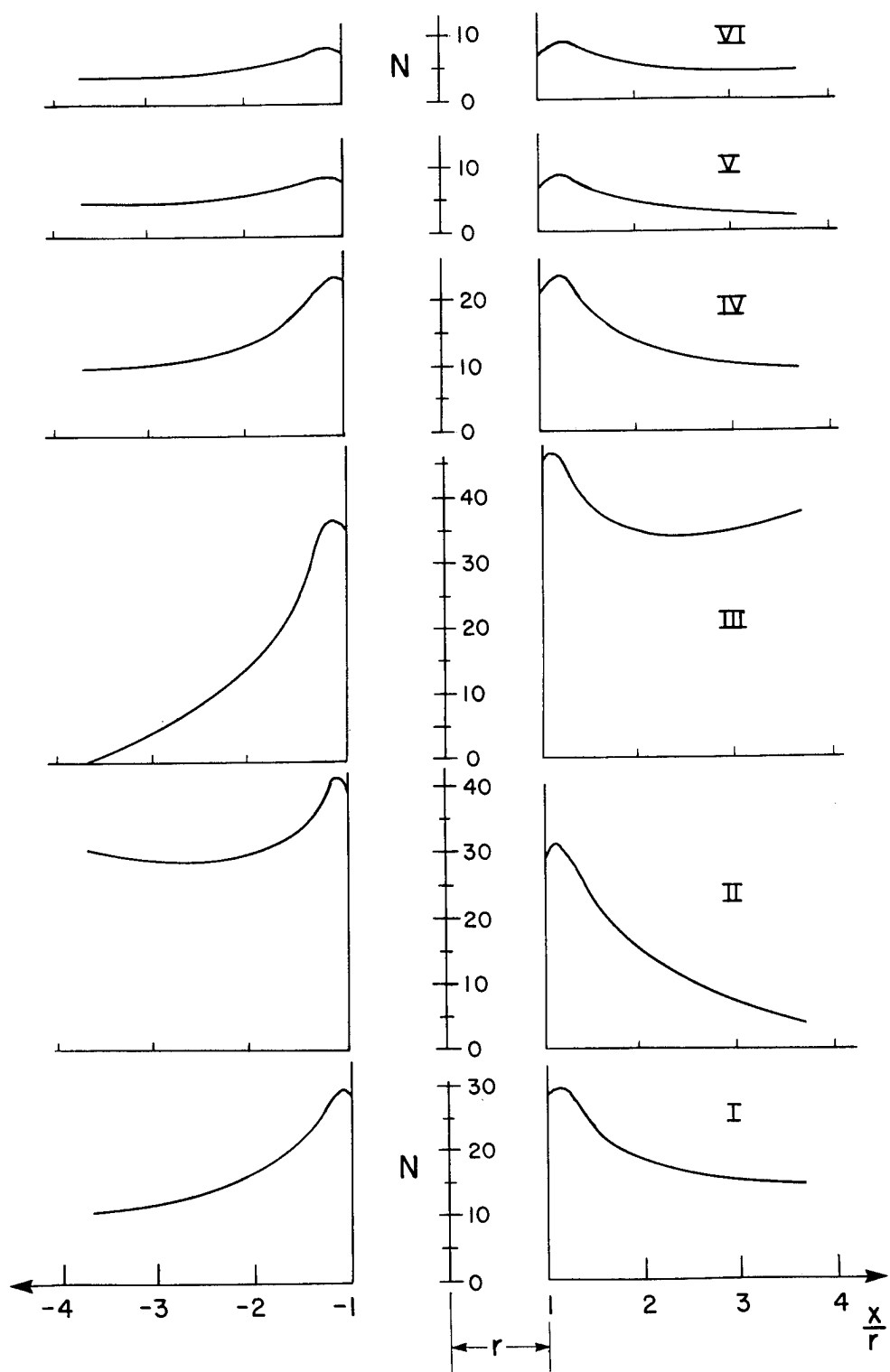
Fig. 14. Fringe order (and thickness change) vs. distance along horizontal centerline; 3/4 inch hole. (a) graphs for each load increment.

Fig. 14(b) Cumulative change of thickness at end of each load increment; 3/4 inch hole.
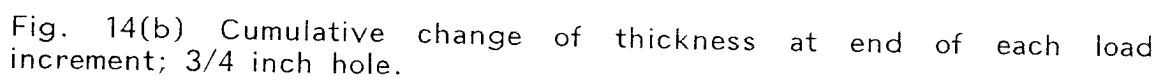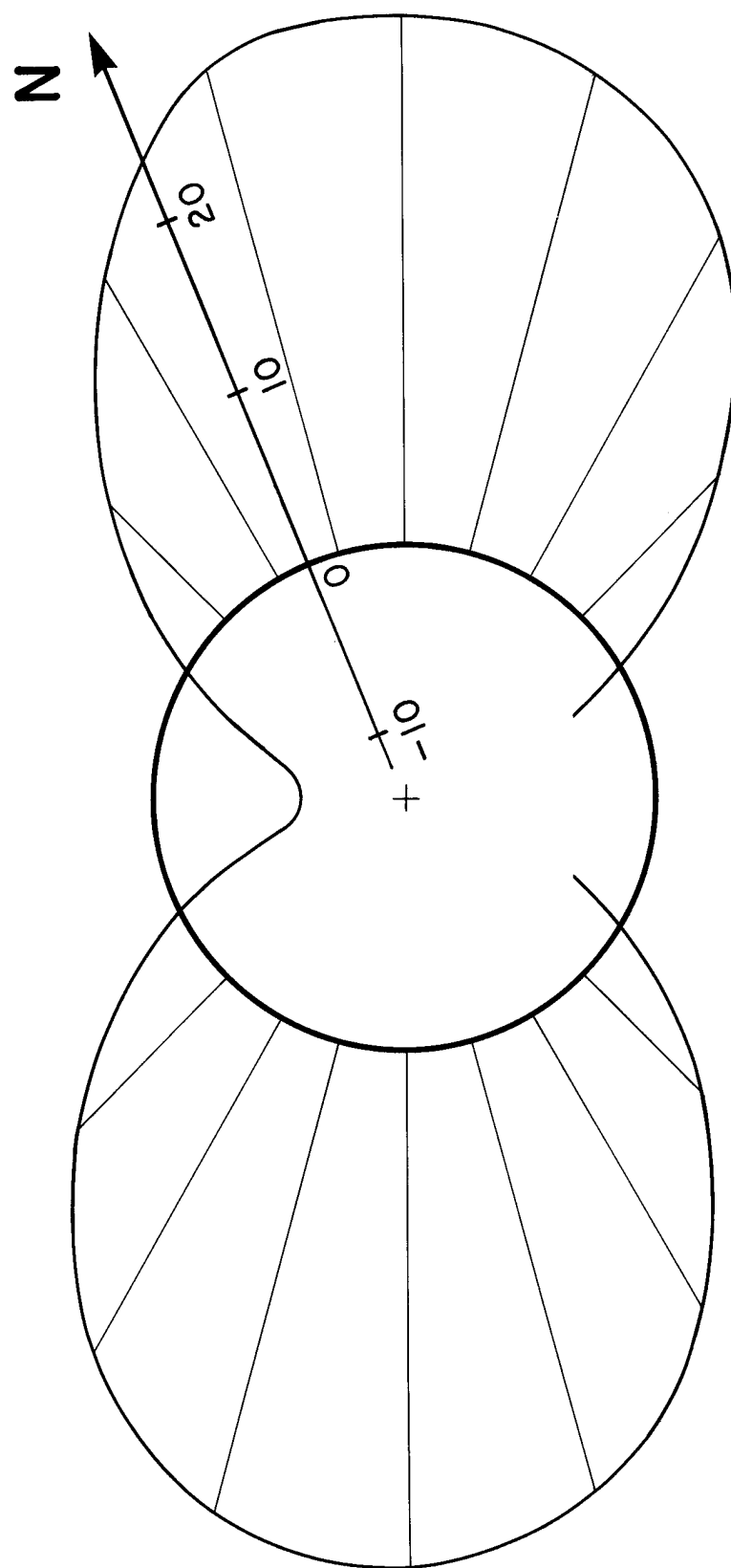
Fig. 14(c) polar graph of change of thickness around perimeter of the hole for first load increment; 1,000 to 16,000 pounds; 3/4 inch hole.

Fig. 15. Fringe order (and thickness change) vs. distance along horizontal centerline; 1/2 inch hole. (a) graphs for each load increment.
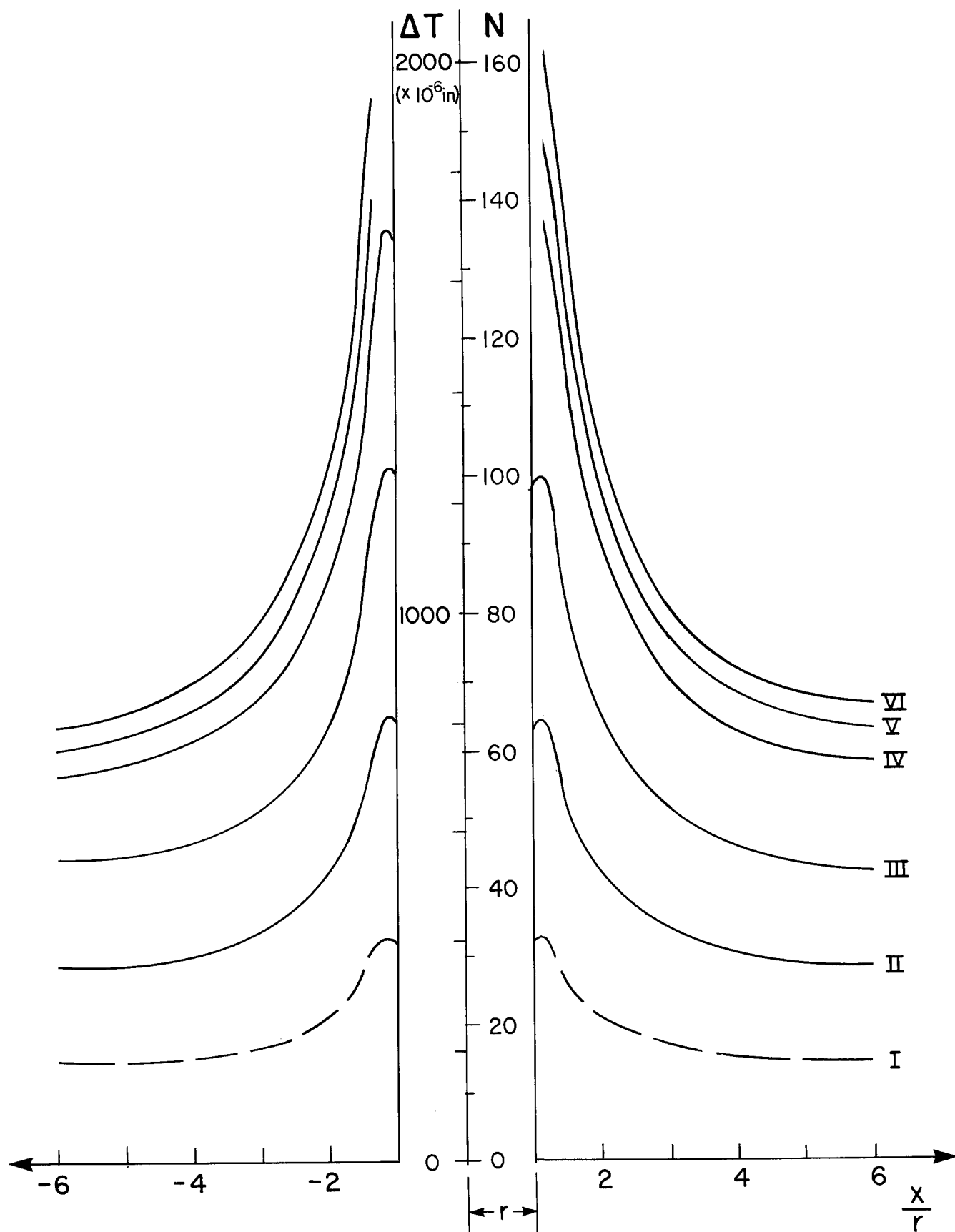
54

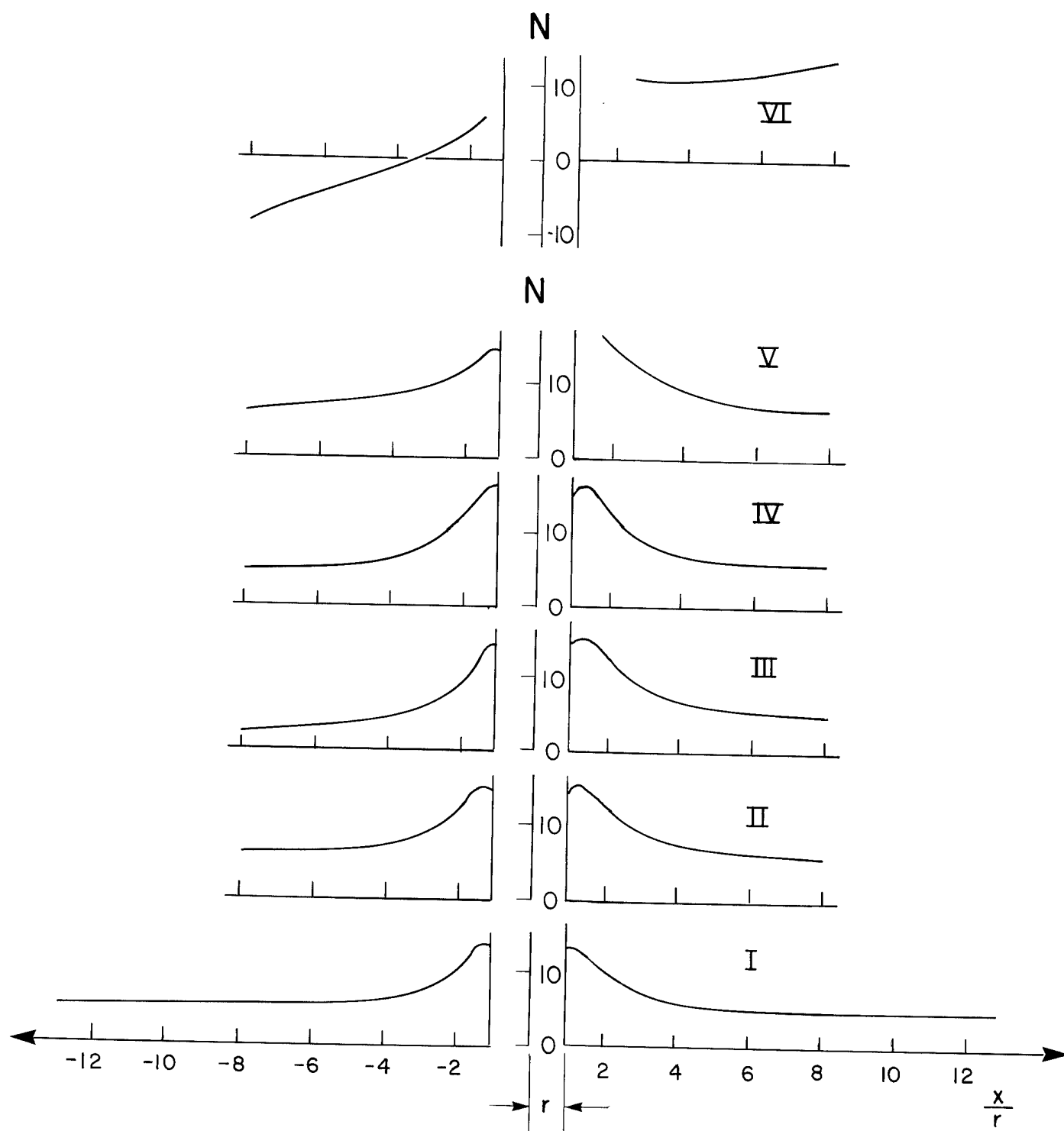Fig. 15(b) Cumulative change of thickness at end of each load increment; 1/2 inch hole.

Fig. 16. Fringe order (and thickness change) vs. distance along horizontal centerline; 1/4 inch hole. (a) graphs for each load increment.
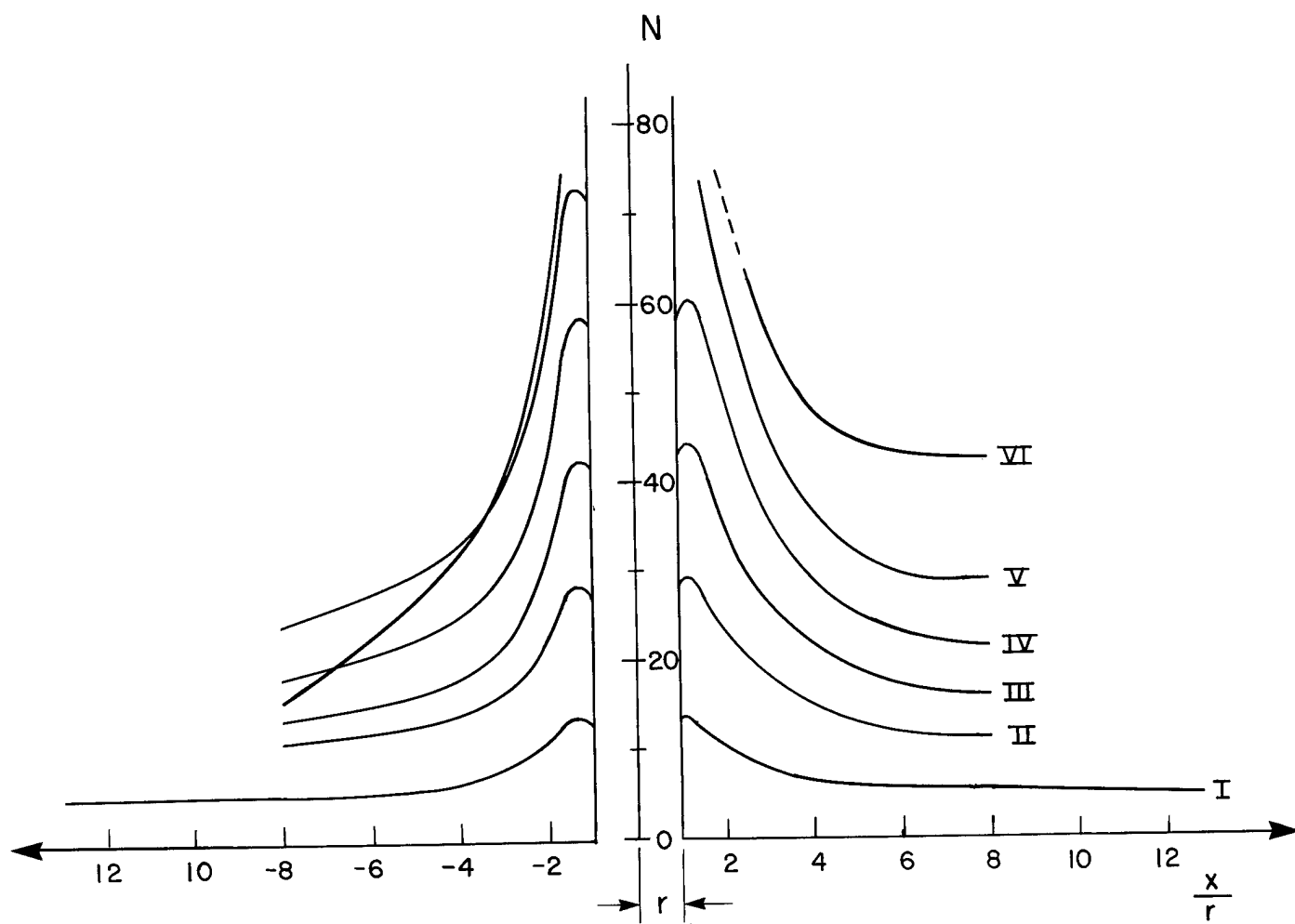
Fig. 16(b) Cumulative change of thickness at end of each load increment; 1/4 inch hole.
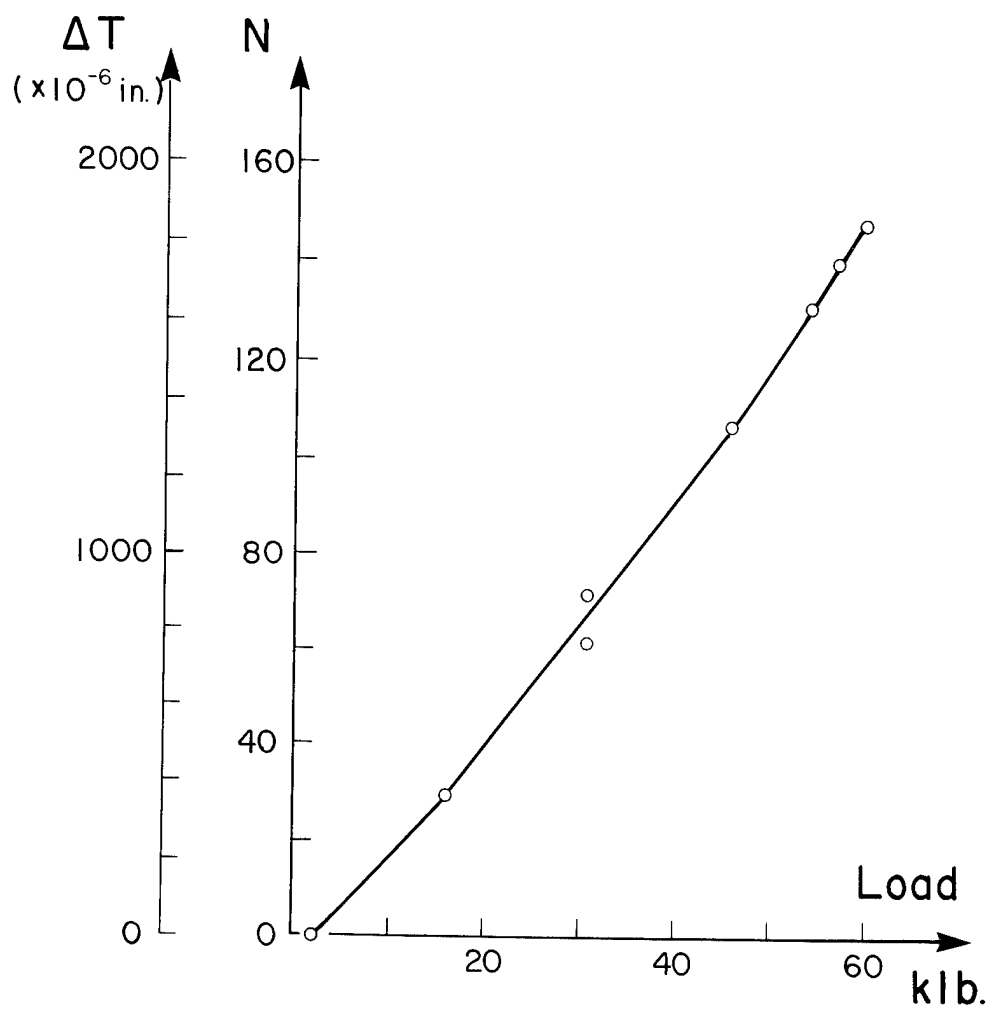
Fig. 17(a). Peak fringe order near hole vs. load for 3/4 inch hole. Lines are drawn through the average of peak fringe orders on left and right side of hole.
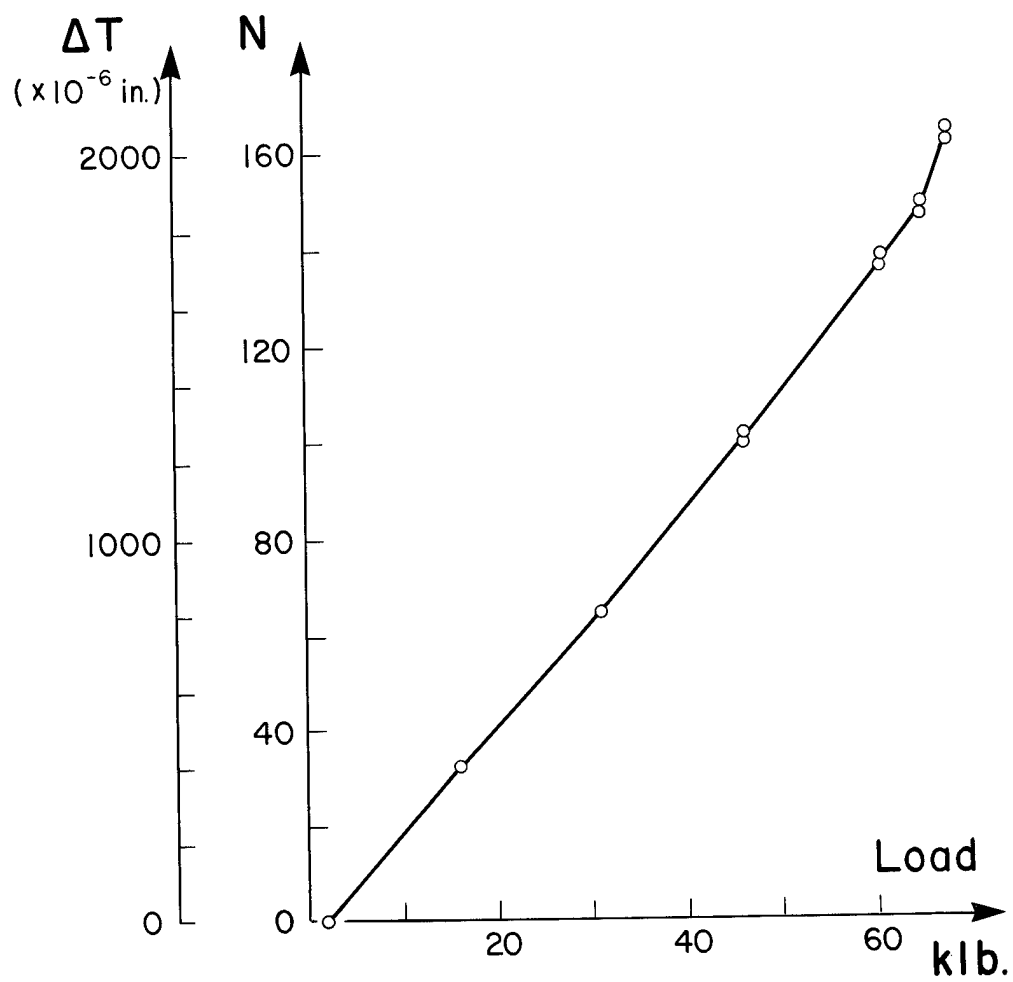
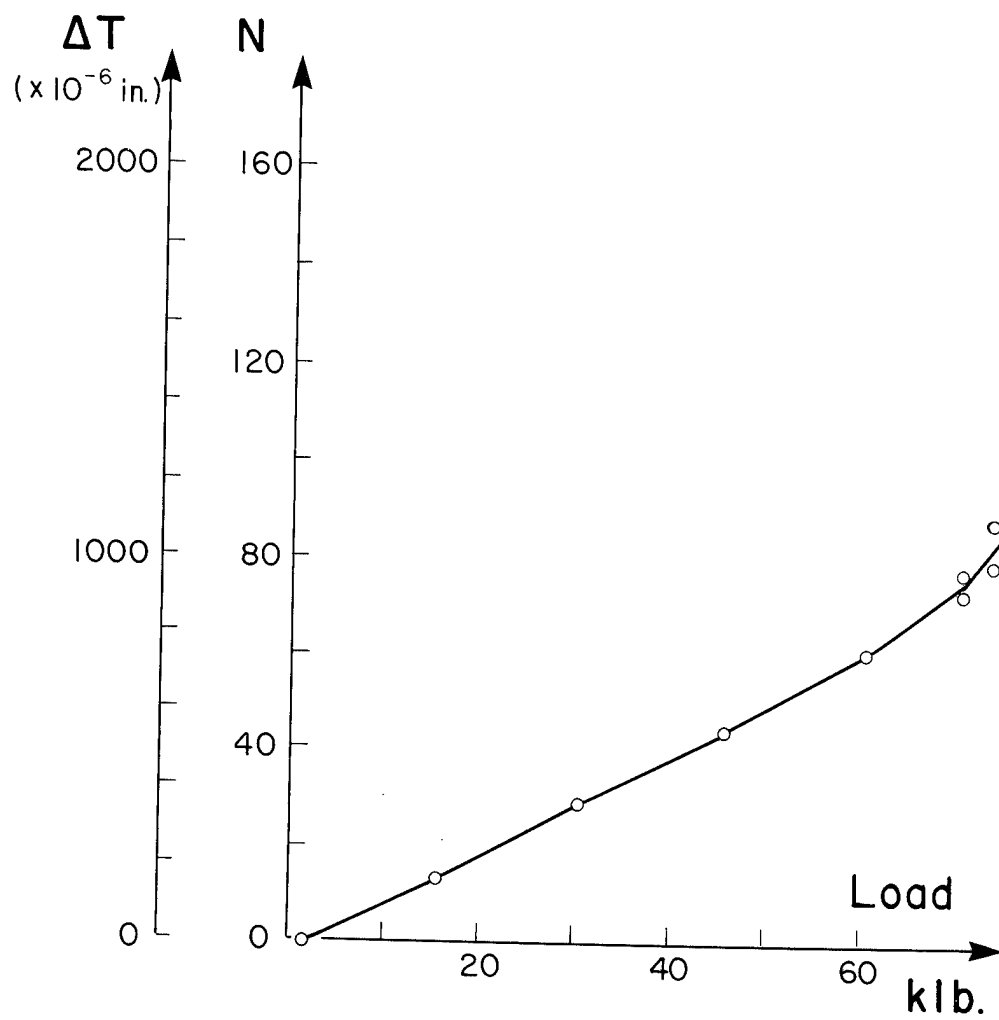Fig. 17(b).   Peak fringe order near hole vs. load for 1/2 inch hole.

Fig. 17(c). Peak fringe order near hole vs. load for 1/4 inch hole.

1. Report No. NASA CR-3989	2. Government Accession No.	3. Recipient's Catalog No.
4. Title and Subtitle Measurement of Displacement Around Holes in Composite Plates Subjected to Quasi-Static Compression		5. Report Date June 1986
		6. Performing Organization Code
7. Author(s) John C. Duke, Jr., Daniel Post, Robert Czarnek, and Anand Asundi		8. Performing Organization Report No.
9. Performing Organization Name and Address Virginia Polytechnic Institute and State University Engineering Science & Mechanics Department Blacksburg, VA 24061		10. Work Unit No.
		11. Contract or Grant No. NAG1-193
12. Sponsoring Agency Name and Address National Aeronautics and Space Administration Washington, DC 20546		13. Type of Report and Period Covered Contractor Report
		14. Sponsoring Agency Code 505-63-11-03

15. Supplementary Notes

16. Abstract

Contour maps of thickness changes were obtained for three quasi-isotropic graphite-epoxy plates with central holes, loaded in compression. Thickness changes were determined for six load increments from nearly zero to within a few percent of the failure load. The largest change of thickness occurred near the hole but not at the boundary of the hole. Below 90 percent of the failure load, the thickness changes were nearly proportional to load. Irregularities of thickness changes occurred in zones of compressive stresses and they were attributed to localized fiber buckling.

A new optical technique was developed to measure thickness changes with high sensitivity. It utilizes a comparatively simple means of holographic interferometry on both sides of the specimen, followed by additive moire to obtain thickness changes as the sum of the out-of-plane displacements. Sensitivity was 12.5×10^{-6} in. per fringe order. The fringe patterns represent thickness changes uniquely, even when specimen warpage and consequent out-of-plane displacements are very large.

17. Key Words (Suggested by Authors(s)) Optical method Change of thickness Quasi-isotropic composites Compressive loads Fiber buckling Holographic interferometry		18. Distribution Statement Unclassified - Unlimited Subject Category 24		
19. Security Classif.(of this report) Unclassified		20. Security Classif.(of this page) Unclassified	21. No. of Pages 66	22. Price A04